USAFETAC/PR--91/020

AD-A260 175

RTNEPH TOTAL CLOUD COVER

VALIDATION STUDY

by

Capt Ronald P. Lowther
Mr Mark T. Surmeier
Capt Richard W. Hartman
Mr Charles R. Coffin
Capt Anthony J. Warren

OCTOBER 1991

APPROVED FOR PUBLIC RELEASE; DISTRIBUTION IS UNLIMITED

USAF ENVIRONMENTAL TECHNICAL APPLICATIONS CENTER

Scott Air Force Base, Illinois, 62225-5438

REVIEW AND APPROVAL STATEMENT

USAFETAC/PR--91/020, *RTNEPH Total Cloud Cover Validation Study*, October 1991, has been reviewed and is approved for public release. There is no objection to unlimited distribution of this document to the public at large, or by the Defense Technical Information Center (DTIC) to the National Technical Information Service (NTIS).

PATRICK J. BREITLING
Chief Scientist

FOR THE COMMANDER

GEORGE M. HORN
Asst Scientific and Technical Information
Program Manager
15 October 1991

A NOTE TO OUR CUSTOMERS--

The authors and editors of this publication welcome feedback, both positive and negative. We value your opinion. Please let us know what you like and do not like about our products. Also, please let us know if your address has changed, or if you wish to receive more or fewer copies of AWS and USAFETAC technical documents in primary distribution. If you need more copies of this document, or if you know of someone else who might be interested in this or other AWS/USAFETAC publications, let us know that, too. Call, write, or FAX:

USAFETAC/LDE,
Scott AFB, IL 62225-5458

DSN 576-6648 Commercial 618 256-6648 FAX 3772

REPORT DOCUMENTATION PAGE

2. Report Date: October 1991

3. Report Type: Project Report

4. Title: RTNEPH Total Cloud Cover Validation Study

6. Authors: Capt Ronald P. Lowther, Mark T. Surmeier, Capt Richard W. Hartman, Charles R. Coffin, Capt Anthony J. Warren

7. Performing Organization Name and Address: USAF Environmental Technical Applications Center (USAFETAC/ECS), Scott AFB, IL 62225-5438

8. Performing Organization Report Number: USAFETAC/PR--91/020

12. Distribution/Availability Statement: Approved for public release; distribution is unlimited.

13. Abstract: In 1983, the United States Air Force Global Weather Central (AFGWC) implemented a new model to map and store an analysis of worldwide cloud-cover derived from surface and satellite data. This model, the designated the Real-Time Nephanalysis (RTNEPH) model, contains analyses of total sky cover, cloud bases, and cloud heights. Studies assessing the accuracy of the RTNEPH database have, up to now, been limited. In this work, the RTNEPH total sky-cover database is evaluated against independent surface observations. Since the RTNEPH algorithm heavily weights available surface observations, this was not a simple task; more than 500,000 independent surface and RTNEPH observations had to be matched and evaluated. Frequency distributions of the differences in these two sources were computed and stratified by latitude, season, time of day (day versus night), and age. Finally, statistical tests were run to obtain quantitative assessments of the results. In general, the RTNEPH total sky cover compared favorably with the surface reports, but there were differences. Certain biases in the RTNEPH were also identified, most notably the underestimation of cloud cover in arctic regions and the poor resolution of RTNEPH in regions where the airways surface observation code is used.

14. Subject Terms: CLIMATOLOGY, METEOROLOGY, WEATHER, CLOUDS, SKY COVER, CLOUD COVER, CLOUD BASES, CLOUD HEIGHTS, WEATHER OBSERVATIONS, ANALYSES, MODELS, COMPUTER MODELS, ATMOPSHERIC MODELS, CLOUD MODELS, REAL-TIME NEPHANALYSIS, RTNEPH

15. Number of Pages: 51

17. Security Classification of Report: Unclassified

18. Security Classification of this Page: Unclassified

19. Security Classification of Abstract: Unclassified

20. Limitation of Abstract: UL

Standard Form 298

PREFACE

In August 1983, the AFGWC Real-Time Nephanalysis (RTNEPH) Model replaced the AFGWC Automated Cloud Analysis Model (3DNEPH). This study evaluates the total cloud cover (TCC) variable of the newer RTNEPH. Many AWS customers have used the RTNEPH TCC without knowing its true accuracy. One such customer (a HQ AWS direct-reporting unit) tasked the USAFETAC Special Projects Section (ECS) for a quantitative evaluation of the TCC variable.

Before developing the approach used in the study, a literature search was conducted with the help of the Air Weather Service Technical Library (AWSTL) to examine previous work on the subject. When little work of any scientific value was found, USAFETAC/ECS devised the approach described in this report to evaluate the accuracy of the RTNEPH TCC variable, then performed and documented the study.

Although only two USAFETAC sections (Special Projects and Environmental Simulation) were directly involved with the study, special recognition is given to the AWSTL and the Data Automation Branch (AD) for their extensive assistance.

CONTENTS

FIGURES

TABLES

1. INTRODUCTION

1.1 Purpose of the Study. The purpose of this study is to evaluate the total cloud cover (TCC) variable in the Air Force Global Weather Center (AFGWC) automated Real-Time Nephanalysis (RTNEPH) cloud model. Because the choice of global databases for comparison is limited, the study primarily compares RTNEPH-derived TCCs with those of nearby independent surface observations. A point study that uses whole sky imager (WSI) data from Malabar, Florida, is included.

1.2 Model History. In 1970, the United States Air Force implemented a program to map and store (in a gridded database) an analysis of worldwide cloud cover. This analysis, designated "3-Dimensional Nephanalysis" (3DNEPH) (Fye, 1978), contained cloud-cover amounts for 15 designated height intervals, as well as total cloud cover. The 3DNEPH has since been altered to improve the quality of the cloud database. In 1983, AFGWC replaced the 3DNEPH with the Real-Time Nephanalysis (RTNEPH) model in an effort to streamline the heavily modified algorithm and more accurately specify data on individual cloud layers (Kiess and Cox, 1988). As part of the new model, diagnostic flags were added to the database; to specify the data sources used in the processing as well as the age of the latest data. The grid of the RTNEPH database is polar stereographic, centered on the poles--see Figures 1 and 2. Spacing between grid points ranges from 33 nm to 13 nm (pole to equator, respectively) and each hemisphere is divided into 64 boxes containing 4,096 data points each. Database frequency is in 3 hourly increments starting with 00Z. In reality, RTNEPH is updated on receipt of new data. Snapshots of this data are taken every 3 hours, about 2 hours after data valid time.

1.3 Previous Studies. Previous research efforts on RTNEPH database quality are limited and mostly unpublished. A few studies compared 3DNEPH/RTNEPH and surface observations; these were limited in scope, applied only to a few selected stations, and were not statistically valid because the RTNEPH and surface observations were not two independent datasets (RTNEPH incorporates available surface observations in its analyses). Other studies merely focused on revealing certain strengths and weaknesses of RTNEPH. Also, most previous articles provide only qualitative information; they do not specify the level of accuracy of the total cloud-cover analysis. For these reasons, along with the operational requirement for knowing the quantitative precision of the RTNEPH data, USAFETAC was prompted to perform this large-scale statistical study using completely independent datasets.

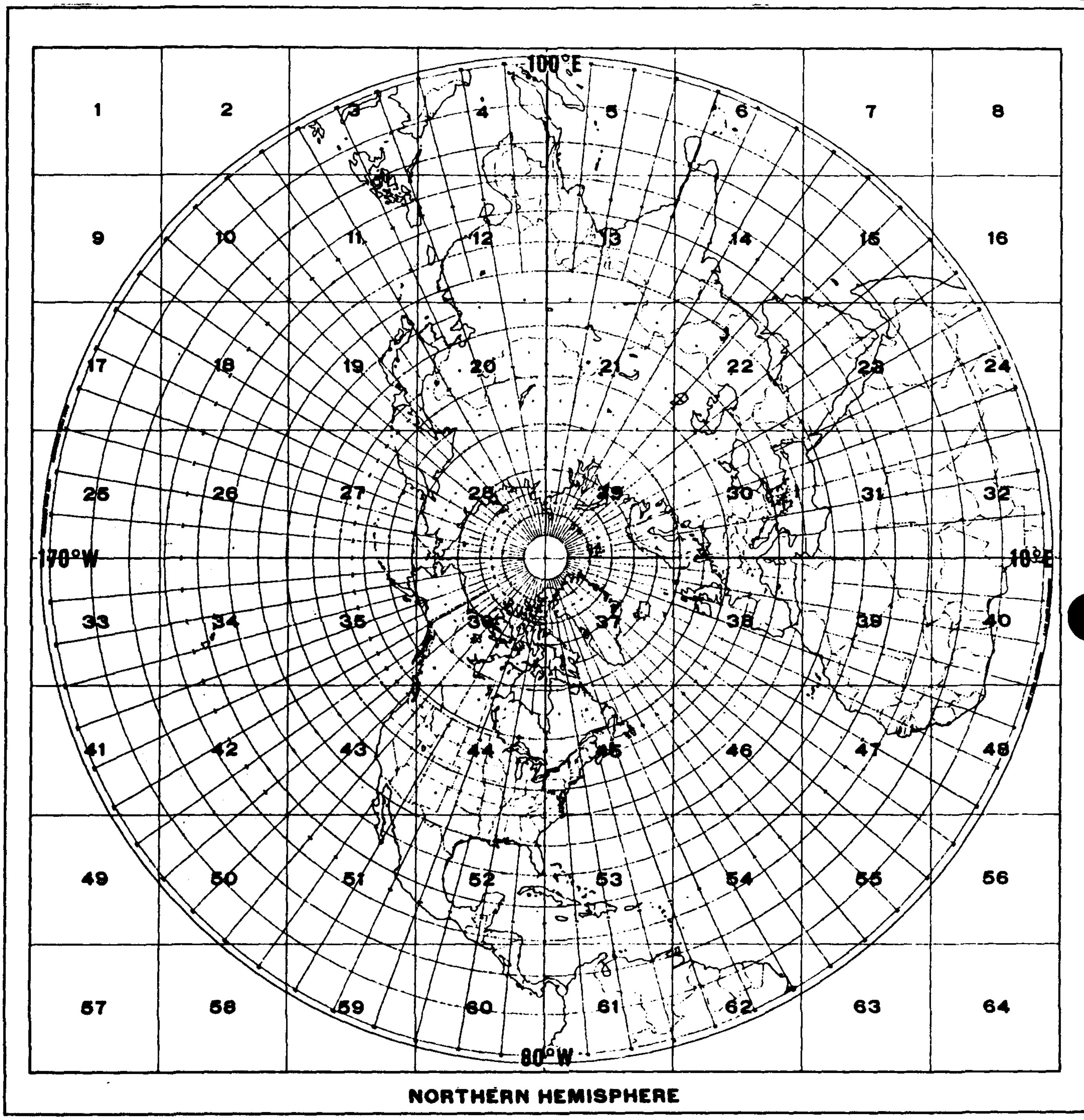

Figure 1. Northern Hemisphere RTNEPH grid over a polar-sterographic projection. Corner boxes are not used.

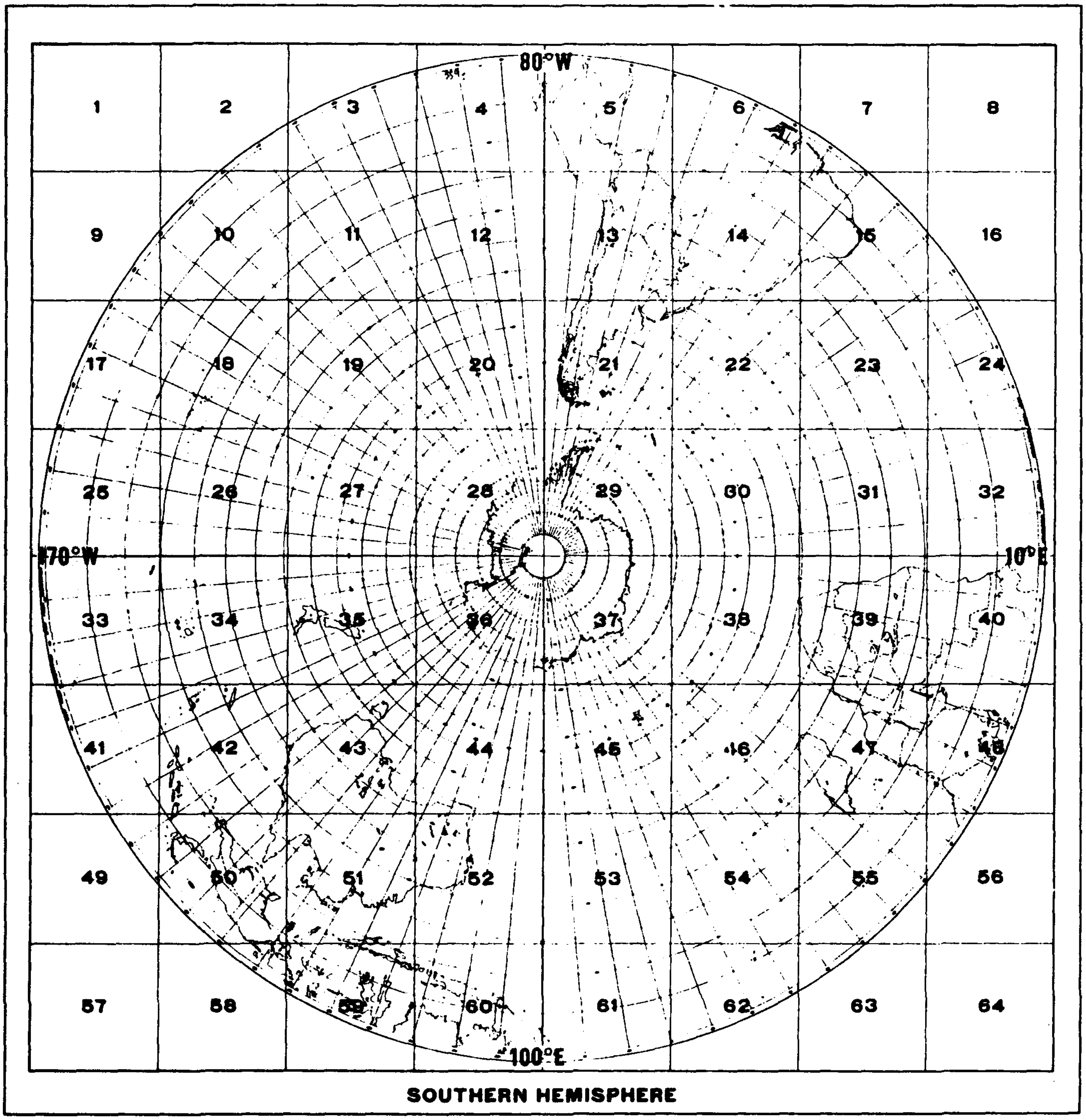

Figure 2. Southern Hemisphere RTNEPH grid over a polar-sterographic projection. Corner boxes are not used. Add 100 to the box numbers shown.

2. METHODS OF ANALYSIS

To evaluate the total cloud-cover database, we compared 5 years (1985-89) of RTNEPH analyses with independent surface observations. Since the RTNEPH algorithm heavily weights available surface observations, RTNEPH output closely resembles them. To conduct a statistically sound study, we had to make sure that the surface observations were not used in the original RTNEPH model processing and were independent of the RTNEPH analyses.

We did this by choosing isolated synoptic reporting stations that did not have any other active reporting stations within 50 NM. This ensured that the RTNEPH model was not using data from other stations within the same grid area and minimized the effect of RTNEPH spreading surface data into the grid area (nearest the surface station) from an adjoining grid area.

The next step involved extracting the RTNEPH data as well as its diagnostic flags. An RTNEPH observation was chosen if the diagnostic flag indicated that no surface station was used in the analysis, or even if surface data was used but was over 3 hours old. Therefore, the corresponding surface observation taken at exactly the same time as the RTNEPH analysis was expected to be independent of the RTNEPH analysis and vice versa. This allows verification of the persistence and satellite analysis of the RTNEPH.

Comparisons of the RTNEPH analyses and these independent surface observations were then stratified and compared by latitude, season, time-of-day, and data age to identify the strengths and weaknesses of the RTNEPH analyses. In addition, statistical significance tests were conducted on the data in order to quantify conclusions concerning the precision of the RTNEPH cloud-cover analysis. Since RTNEPH-based TCC is stored as whole percent and surface-based TCC (from synoptic reporting stations) is reported and stored in octas (eighths of sky coverage), we had to choose a standard. We converted the RTNEPH data into octas (using WMO standards), since the octa is the least-precise reportable value; conversion of octas to whole percent would imply more precision than exists. More than 420,000 such observation pairs were used in the analysis from 168 surface reporting stations (and their corresponding closest RTNEPH grid points). The stations were selected from the following regions; selection criteria included latitude as well as previous USAFETAC data requests for TCC data; see Figures 1 and 2 for RTNEPH box locations. An added value of 100 indicates boxes in the southern hemisphere.

Latitude	Geographic Region	RTNEPH Box #
Polar	Northern USSR/Finland	29
Mid-Latitude	Korea/Eastern China	20
Mid-Latitude	Iraq/Turkey/Syria	22
Mid-Latitude	Chile/Argentina	121
Mid-Latitude	New Zealand	135
Tropical	Western Africa	40
Tropical	Eastern Pacific Islands	60
Tropical	Colombia/Venezuela	61

3. ASSUMPTIONS AND LIMITATIONS OF THE DATA

3.1 Ground Truth. The assumption was made that the surface observations represent "ground truth." Since clouds are between 1 and 2 orders of magnitude closer to ground observers than they are to the polar-orbiting meteorological satellites that feed the RTNEPH model, the resulting determination of cloud cover doesn't always agree. Figure 3 shows the inherent differences in viewing perspectives between earth- and space-based observations. For the surface observer, clouds closer to the horizon increase the apparent sky cover because the sides of the clouds (not just their bases) obscure the celestial dome. For space-based viewing, the cloud scenes are projected onto a flat surface; at ground level, they are projected unto a curved surface. In reality, the satellite and surface sky cover amounts each represent a different physical phenomenon. A rough correction can be made to the surface observation if one knows the heights and angular location of the clouds (Snow, 1990). Since this information is not recorded by observers, we are unable to correct for it. The net effect is that surface-based observations should, on average, be cloudier than the corresponding space-based observations. However, since surface data is reported to the nearest octa, this effect should be small. It is reasonable to assume that the surface observing bias will rarely be greater than one octa, and in most cases, less.

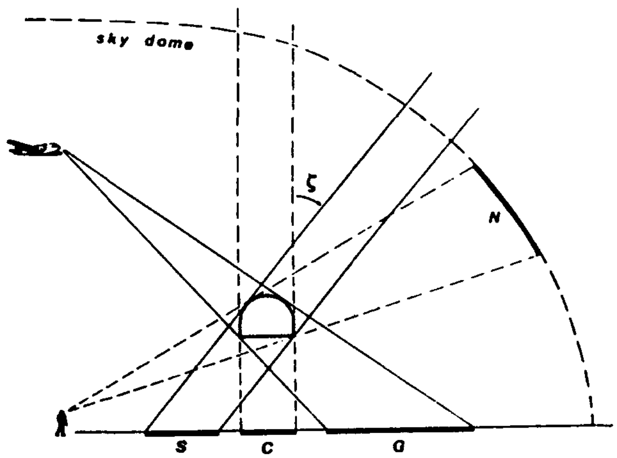

Figure 3. Cloudiness quantifications. S, apparent cloud cover; C, cloud cover; G, ground cover; N, sky cover. ξ is view angle. Heavy line segments depict areas masked from view by cloud (Snow, 1990).

3.2 Observer Subjectivity. The subjectivity of the observer also contributes to error. Differing skill and experience levels of human observers, as well as differences in reporting practices around the world, result in subjectivity and inconsistency. In this study, we are combining large numbers of observations from various locations. This, along with random sampling, should cancel out observer-induced biases. An exception is the nighttime observational bias, which one would expect to be common to all locations. Various studies have reported that observers tend to under-report cloud cover at night; that is, mean cloud-cover on nights with a full moon can vary up to 20% from nights with a new moon. By stratifying the data day/night, we should be able to determine the significance of this bias.

3.3 Diagnostic Flags. The assumption is also made that the RTNEPH diagnostic flags accurately show whether or not surface reports were processed for a particular analysis. While this is a significant assumption, examination of TCC frequency distributions of both the RTNEPH and surface reports from various selected stations lead us to believe the flags are operating properly.

3.4 Bogusing Effects. Bogusing refers to the manual subjective adjustment of the TCC amount by AFGWC analysts if a visual inspection of the satellite imagery appears to conflict with the computer analysis (Kiess and Cox, 1988). Bogusing tends to smooth an area of clouds that may or may nor be "good." It is unknown where or when bogusing occurred, but AFGWC suggests most is done in the mid-latitudes. We should therefore expect the best agreement between RTNEPH and the surface observer in this latitude band. In any case, bogusing is an integral part of the RTNEPH analysis and resulting database; it should only improve an analysis.

4. STRATIFICATIONS

4.1 Stratification by Latitude Band. In order to provide a thorough study of the database, we stratified the data into several categories. The initial stratification divided the global station coverage into different latitudinal bands. The breakdown of the bands is as follows: Polar Latitudes (poleward of 70°), Mid-Latitudes (30° - 60°), and Tropical Latitudes (15° S - 15° N). The regions were broken down this way because of known RTNEPH deficiencies, such as ice/cloud distinctions in arctic areas and satellite data underlap in tropical areas.

4.2 Season Stratification. The second stratification was by season (winter, spring, summer, and autumn). This breakdown was accomplished for each region in addition to the combined or global data set.

4.3 Day/Night Stratification. The third stratification involved grouping the observations by day and night. For this study we considered a mid-latitude location, arbitrarily selecting RTNEPH Box 22 (Middle East). We examined only stations in adjoining time zones to ensure they all were experiencing daylight or nighttime conditions for the pre-set hours. Six-hour intervals were studied in each case. The hours of 0900-1500L (0600-1200Z) depicted daylight, while 2100-0300L (1800-0000Z) depicted nighttime. These time intervals were chosen to avoid the optical effects of dawn and dusk. Although we limited this stratification to one region, we anticipate a high global consistency of day/night bias applies to non-arctic regions. Day and night stratification in the arctic regions was not done because no practical meteorological benefit was expected due to the summer day and winter night tendencies.

4.4 Data Age Stratification. The final stratification was for "data age," which refers to the difference between the latest data observation time (from whatever source--satellite, surface, aircraft, etc.) and the RTNEPH reference time (the official time of the analysis). Because of the non-symmetrical meteorological satellite constellation, and because of the highly latitude-dependent characteristics of polar orbits, data age varies greatly. We limited this study to data up to 24 hours old, since most falls within this category. In addition, this test was only accomplished for the global stratification. We stratified data age with the following time categories: 0-3 hours, 4-6 hours, 7-12 hours, 13-18 hours, and 19-24 hours.

5. ANALYSIS

5.1 Regional and Seasonal Stratifications. The first two stratifications (region and season) were combined for the analysis. The global data set, and those of the individual regions, were broken down by season. For this study, we examined both the whole population and random samples of 5,000. Use of multiple random samples provides better confidence in the results of statistical tests and ensures our conclusions are robust. (A robust estimate is one that is not restricted to a particular sample or dependent upon a key assumption.) Figures 4-7 give cloud-cover frequency distributions for the population as well as two random samples of 5,000 for RTNEPH reports in the polar latitudes. These figures and statistical tests show that this sample size is sufficient to represent the overall population.

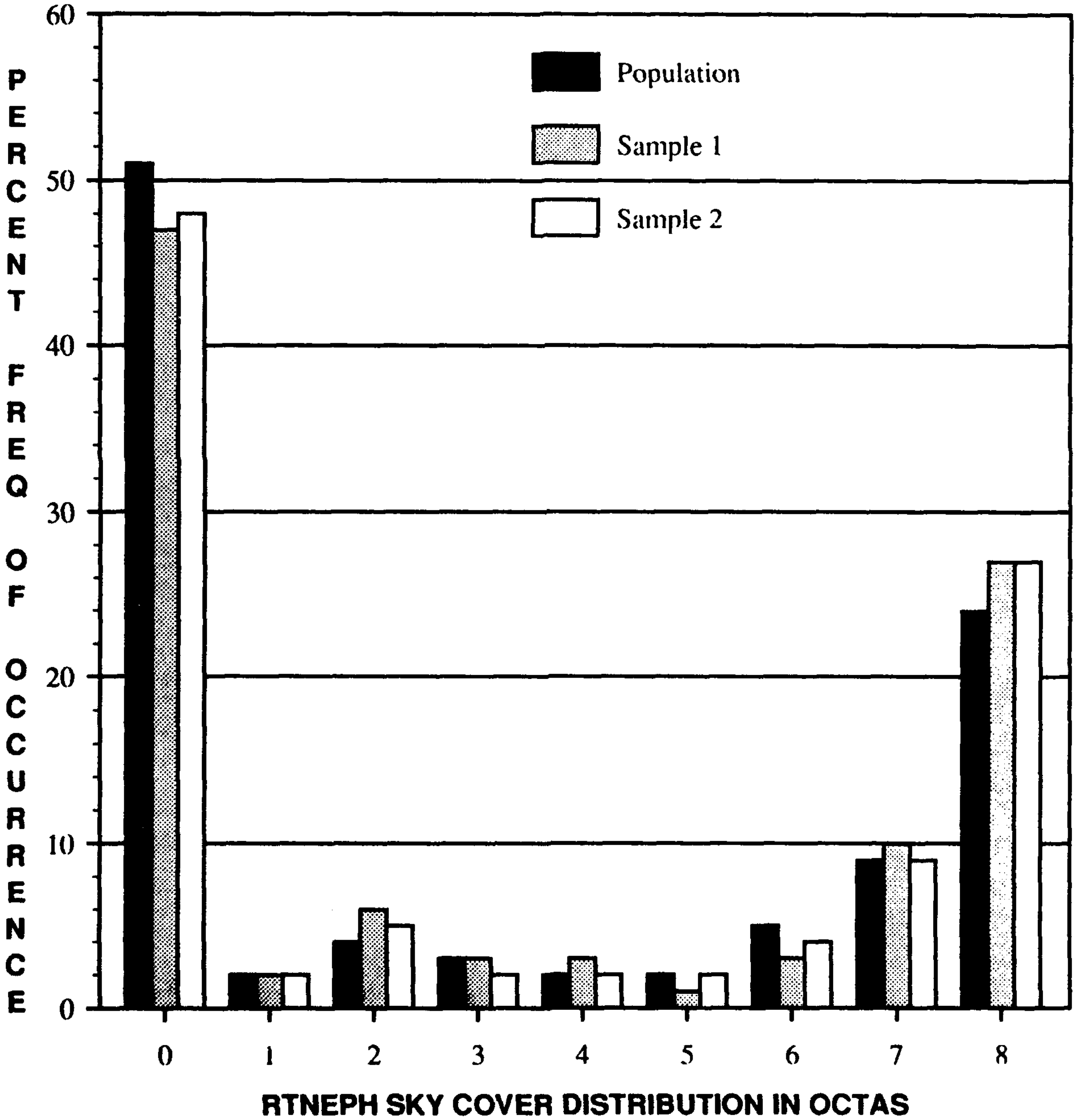

Figure 4. Difference Between RTNEPH Reports for Different Sample Sizes, Polar Latitudes, Winter.

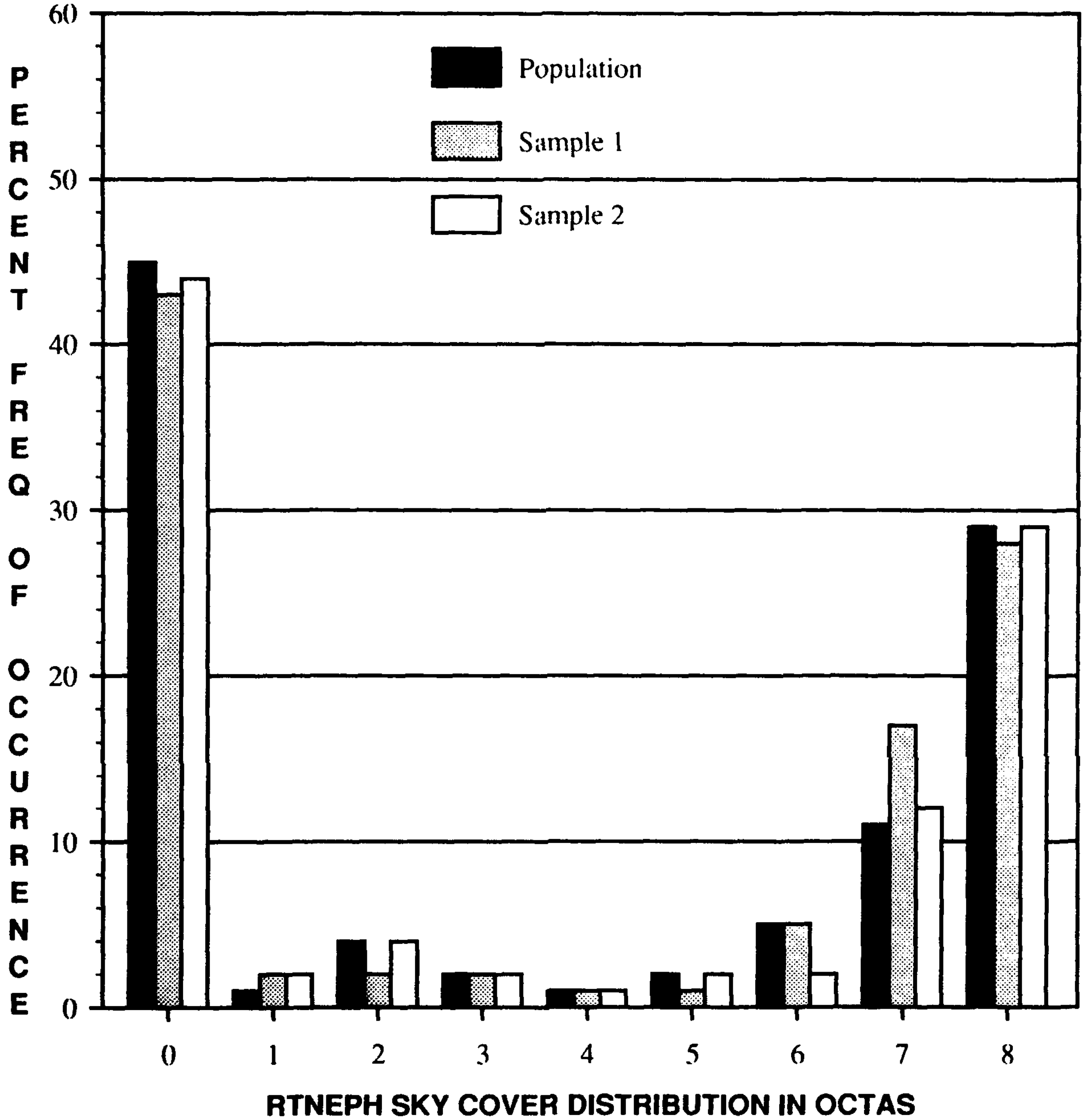

Figure 5. Difference Between RTNEPH Reports for Different Sample Sizes, Polar Latitudes, Spring.

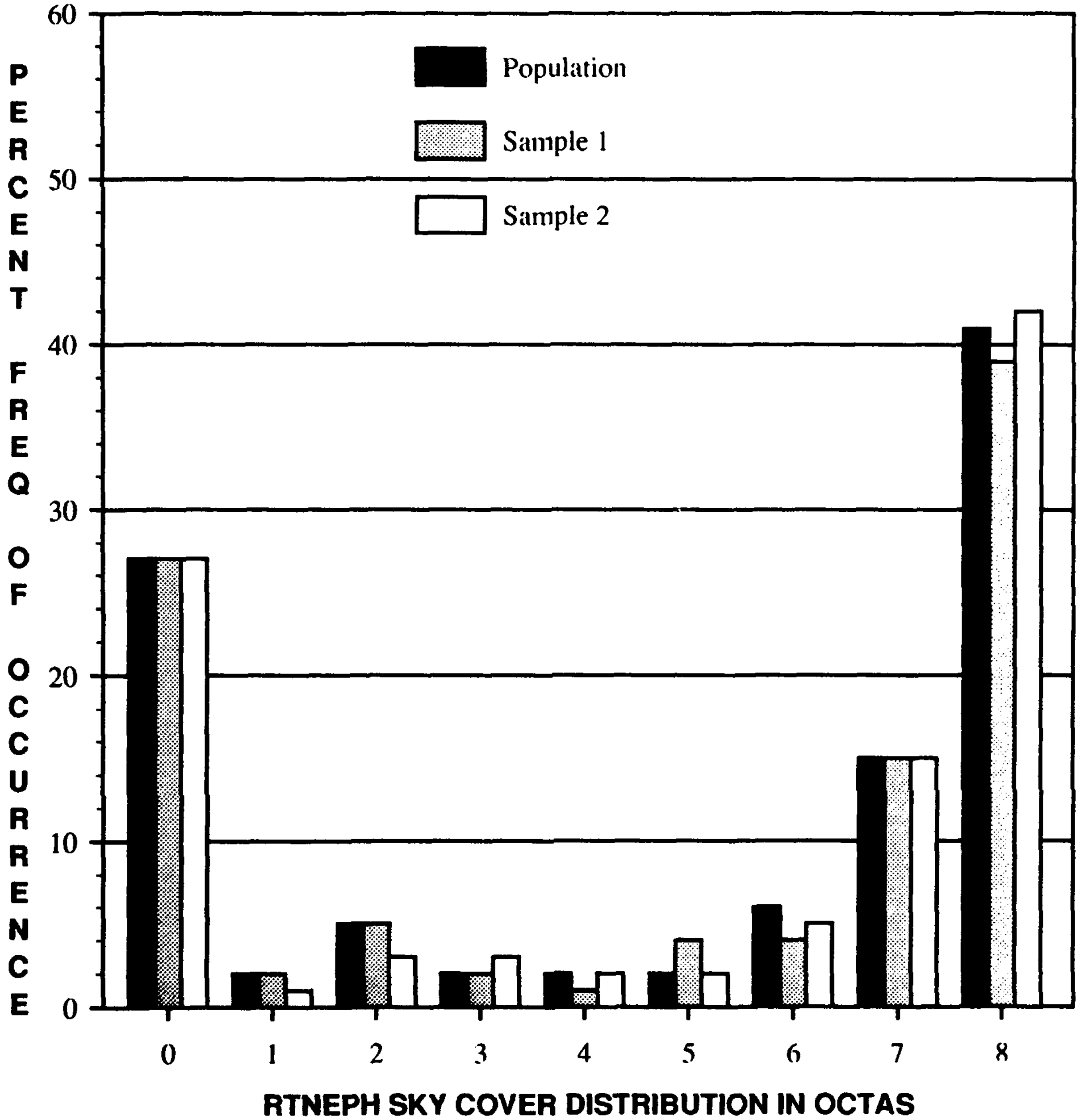

Figure 6. Difference Between RTNEPH Reports for Different Sample Sizes, Polar Latitudes, Summer.

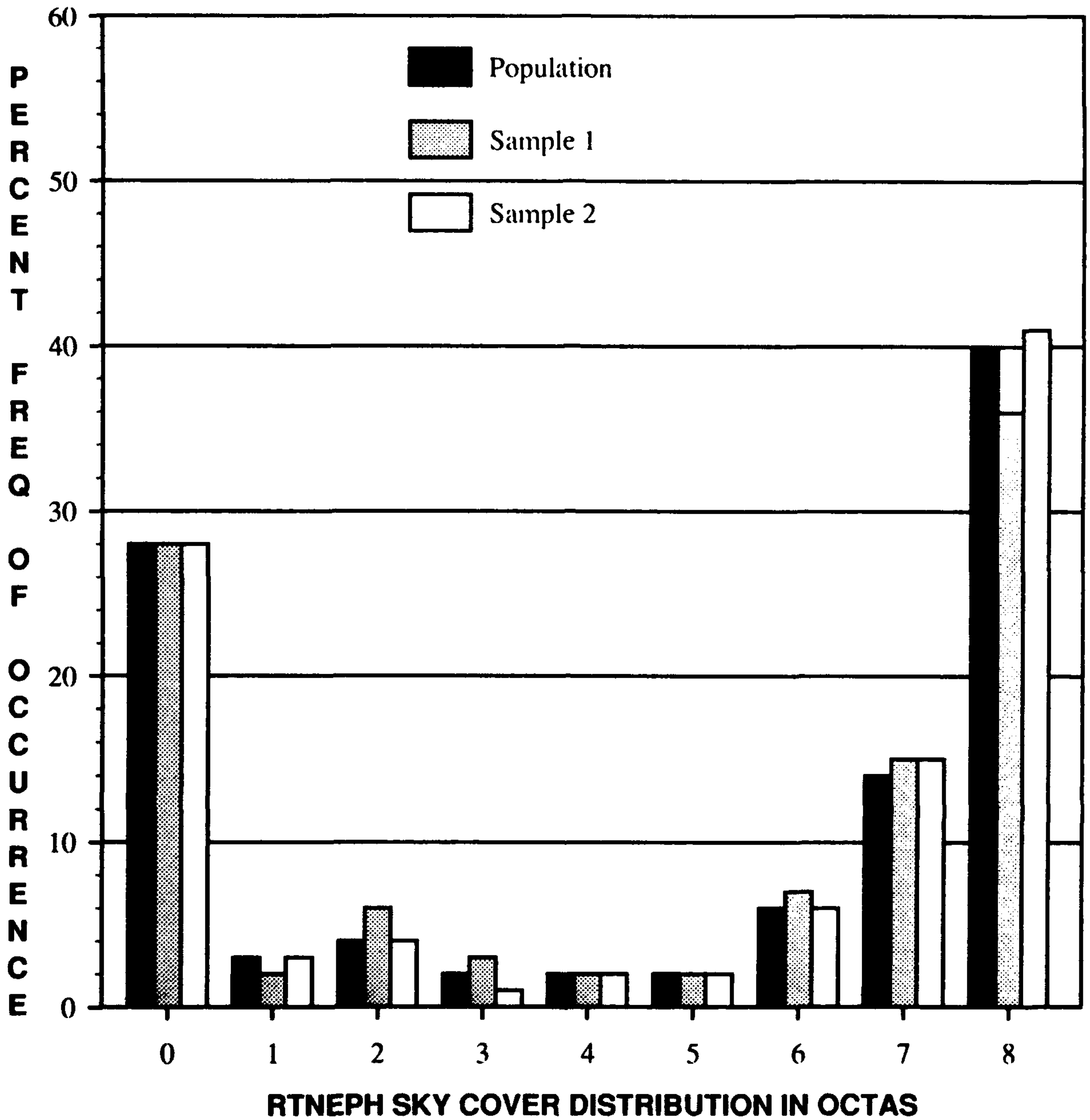

Figure 7. Difference Between RTNEPH Reports for Different Sample Sizes, Polar Latitudes, Autumn.

Frequency distributions of the differences between the paired values (RTNEPH value minus the surface observation value) were generated for each stratification. As mentioned in Section 2, the surface observations were recorded in synoptic code, offering a resolution in octas. The RTNEPH percentage values were therefore converted to octas using WMO conversion standards.

After the distributions were calculated for the global and regional databases, the results were combined and plotted on a single graph for each season (Figures 8-11). As expected, each distribution has a well-pronounced peak at the zero interval. The percentage of observations within 1 and 2 octas of each other are summarized in Tables 1 and 2, respectively. These percentages quantify the precision of the RTNEPH analysis.

TABLE 1. Percent of RTNEPH Total Cloud Cover Observation within 1 Octa (by Region).

SEASON	Global	Polar	Mid-Lat	Tropical
WINTER	59	47	67	57
SPRING	58	49	65	54
SUMMER	64	58	69	58
AUTUMN	64	58	70	60

TABLE 2. Percent of RTNEPH Total Clouds Cover Observation within 2 Octas (by Region).

SEASON	Global	Polar	Mid-Lat	Tropical
WINTER	69	59	76	71
SPRING	69	60	75	68
SUMMER	74	68	79	69
AUTUMN	74	68	79	71

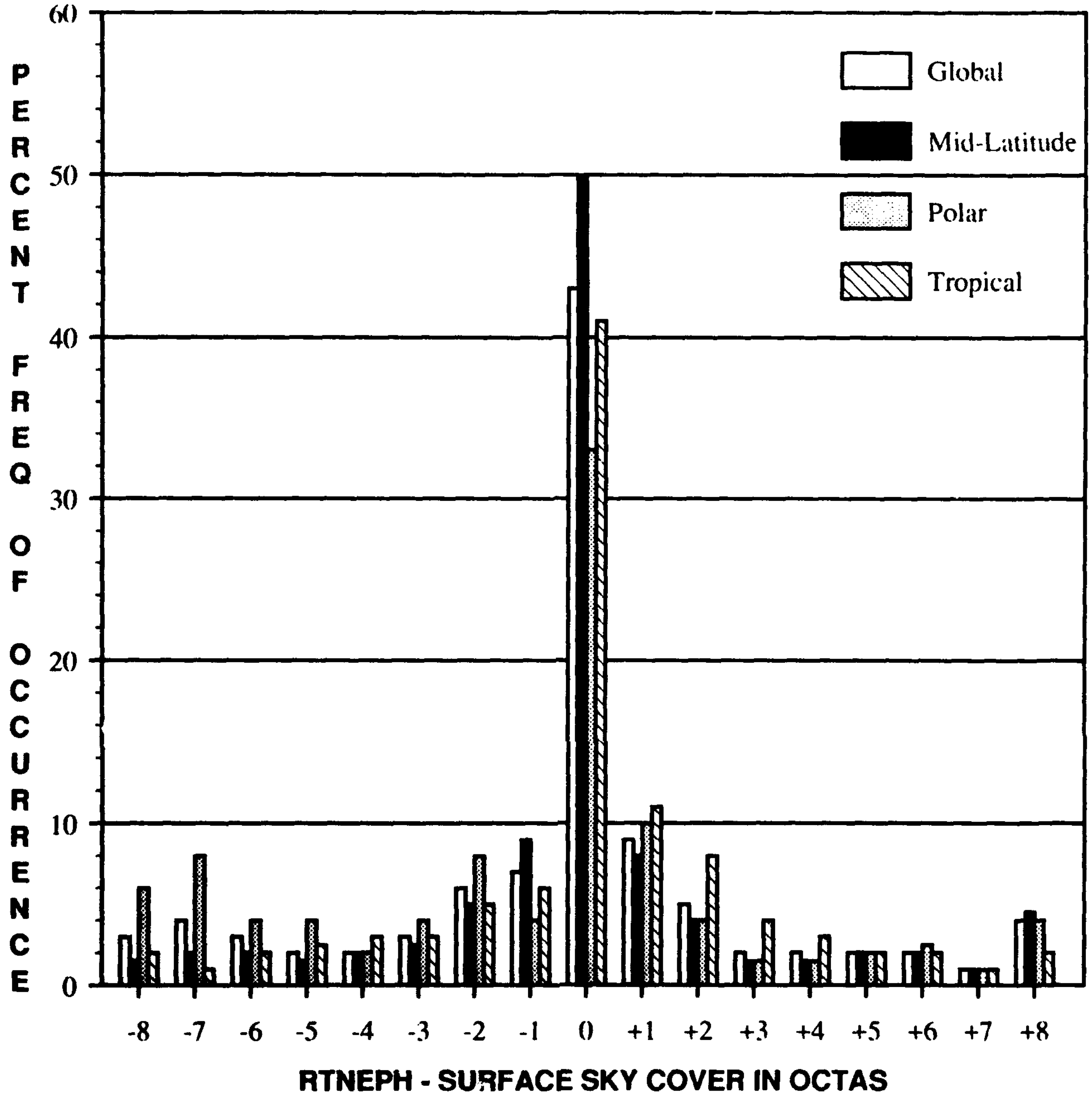

Figure 8. Latitude Comparison of RTNEPH minus Surface Observations, Winter.

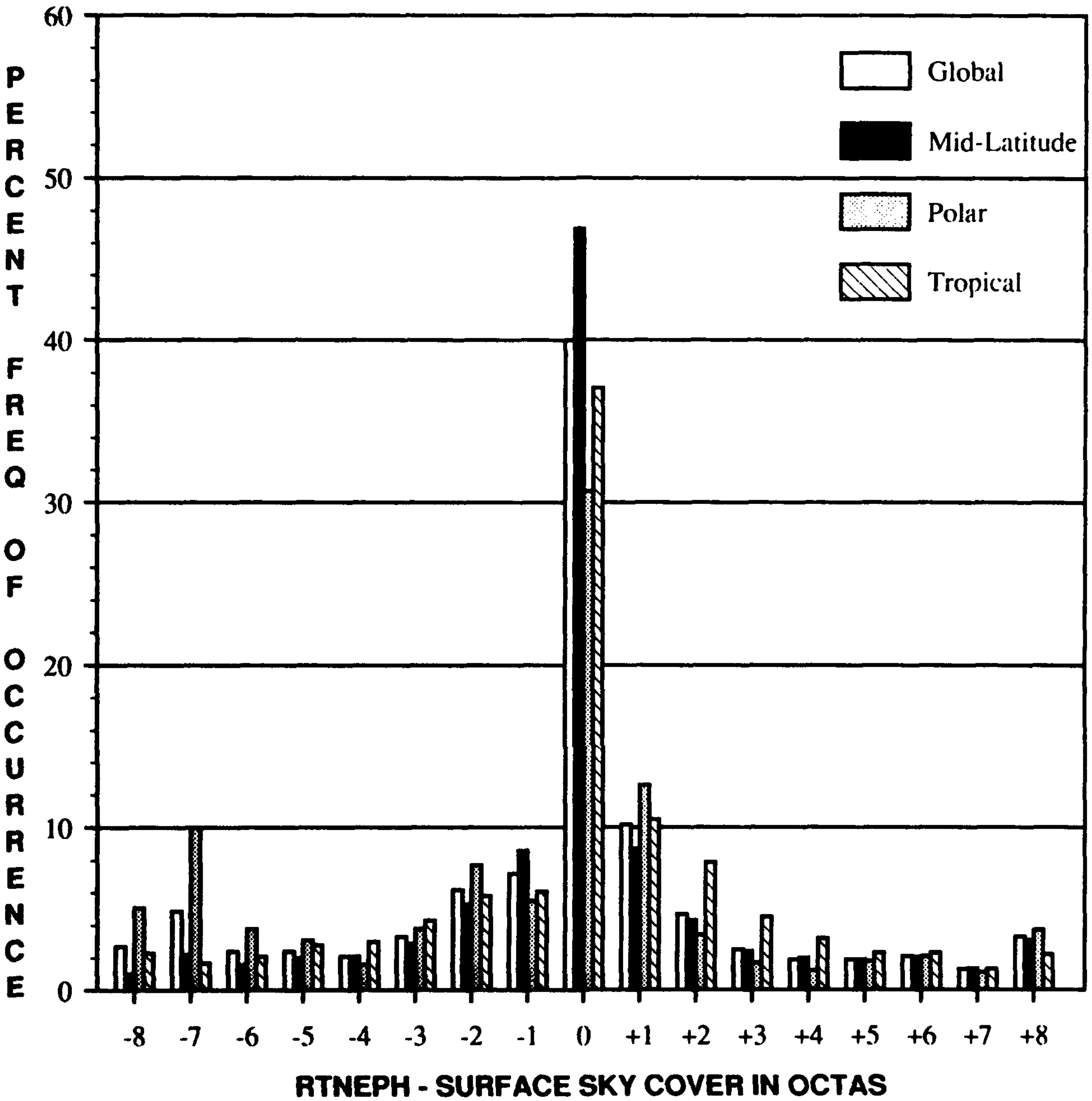

Figure 9. Latitude Comparison of RTNEPH minus Surface Observations, Spring.

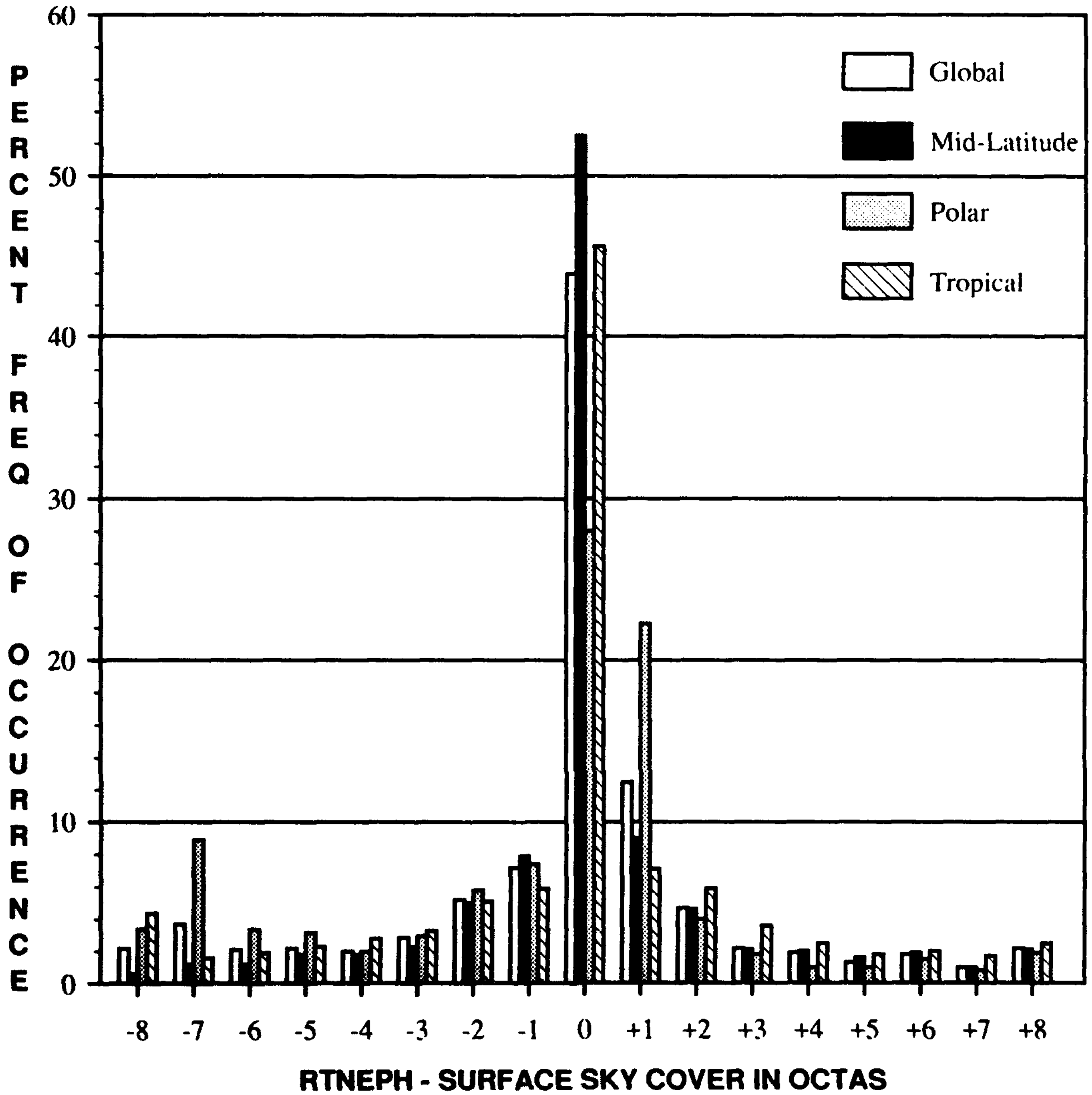

Figure 10. Latitude Comparison of RTNEPH minus Surface Observations, Summer.

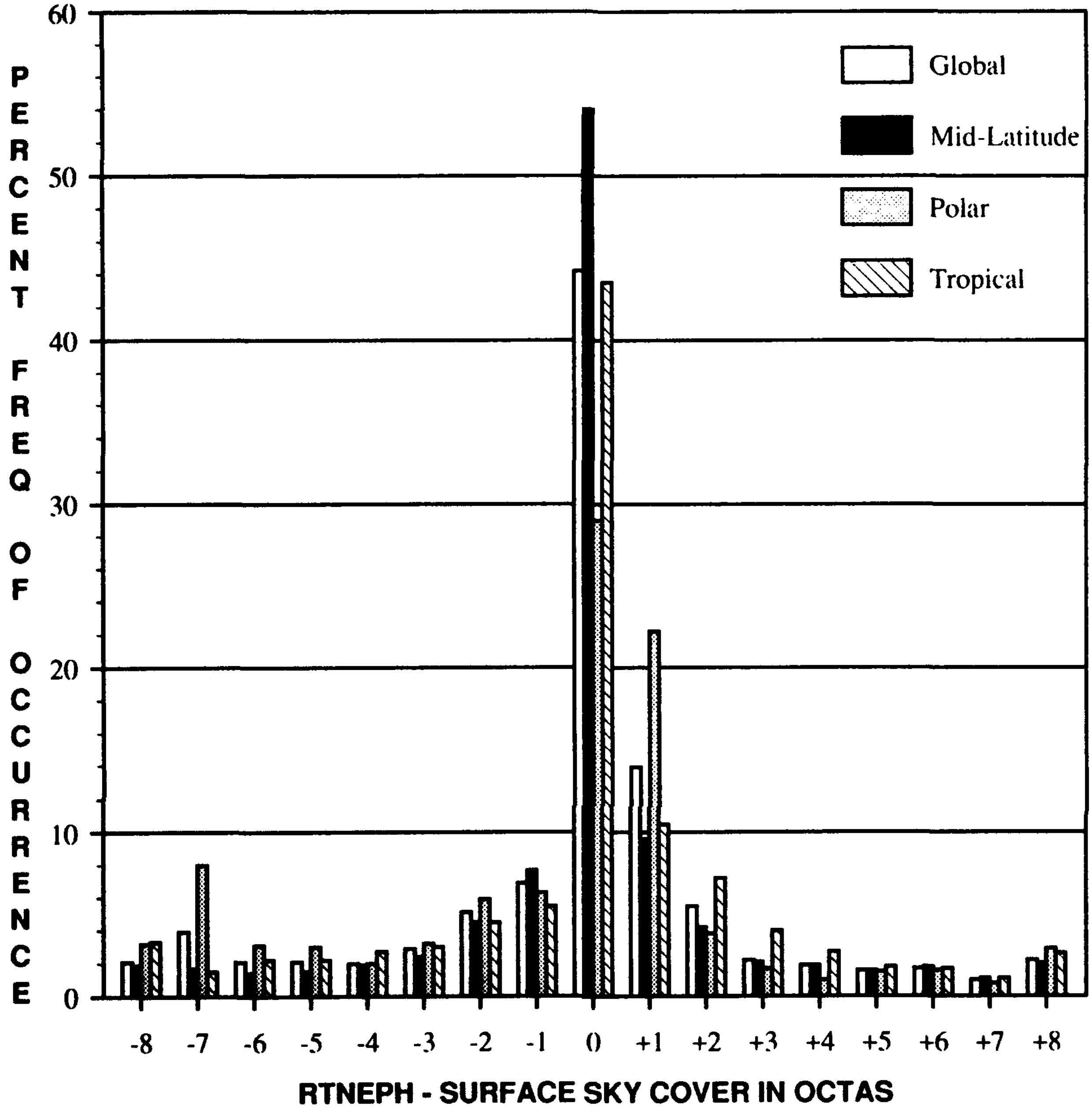

Figure 11. Latitude Comparison of RTNEPH minus Surface Observations, Autumn.

As shown in Tables 1 and 2 and Figures 8-11, the surface observations and the RTNEPH agree most of the time. The largest discrepancy occurs in the polar regions, especially during winter and spring. Note the small, persistent peak over the -7 interval. (A negative difference is the result of the observer recording more cloud cover than the corresponding RTNEPH analysis). Persistent ice or snow cover and low stratus are often indistinguishable in infrared satellite imagery (visual data is not used over ice- or snow-covered areas) due to lack of temperature and background color contrast; this may well be the source of these errors. As a result, the polar discrepancy affects the global distribution.

5.2 Day/Night Stratification. Nighttime conditions affect both the satellite's and ground-based observer's abilities to determine cloud cover accurately. To evaluate this potential bias, an area in the mid-latitudes (RTNEPH Box 22) was selected; we applied the same differencing technique between the RTNEPH and surface observations as discussed earlier. It should be noted that RTNEPH was updated early in the day/night period (by 1000/2200L) with DMSP satellite passes; the rest of the period represents persistence. No matter what region of the world is chosen, each day/night period would only be updated once (except for polar regions), and the rest of the day/night period would represent persistence.

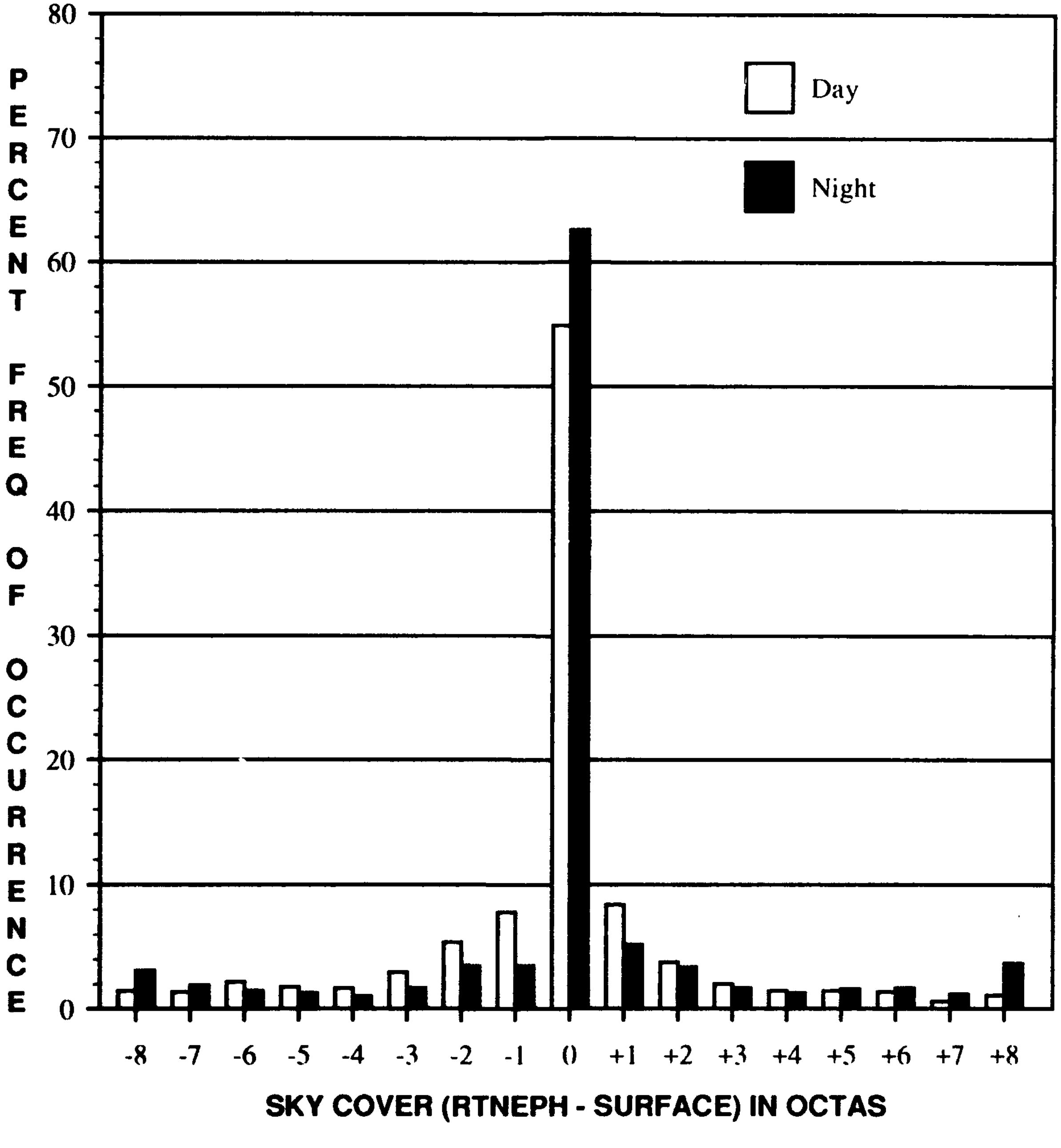

Figure 12. Comparison of Day/Night RTNEPH minus Surface Observations, mid-Latitudes, Winter.

Separate plots were prepared for daytime and nighttime observations. Figures 12-15 depict the seasonal distributions for this stratification. They indicate more agreement at night than during the day. We suspect that this is just as likely to indicate that RTNEPH and surface reports are similarly biased by the disabling effects of darkness (the satellite has no visible imagery at night) as it is to imply that both are more accurate at night. Although both show more clear observations at night, this does have physical support; convective clouds often dissipate soon after dark. Frequency distributions were plotted for both the RTNEPH and surface observations comparing the day versus night hours (Figures 16-19 and 20-23).

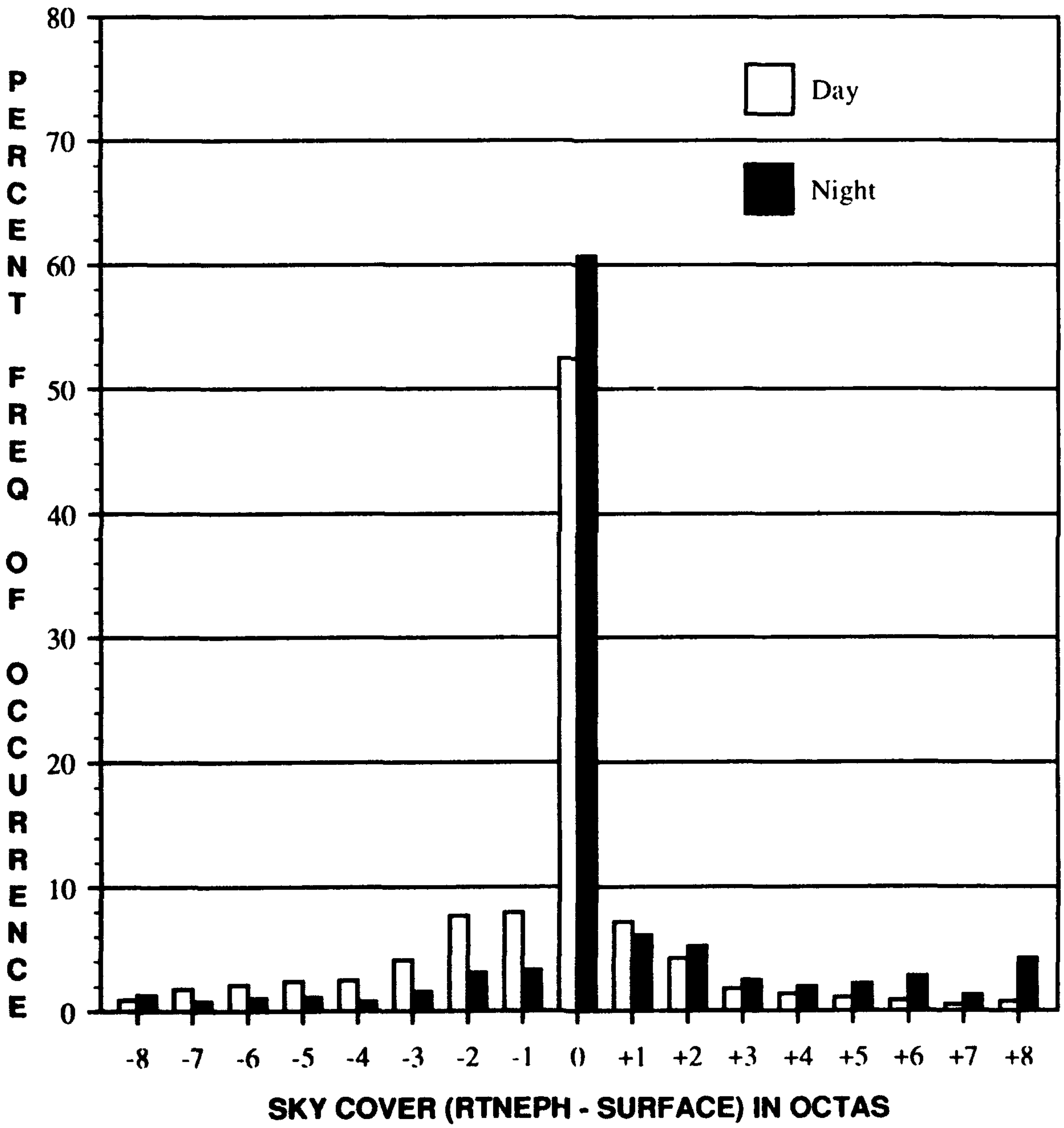

Figure 13. Comparison of Day/Night RTNEPH minus Surface Observations, mid-Latitudes, Spring.

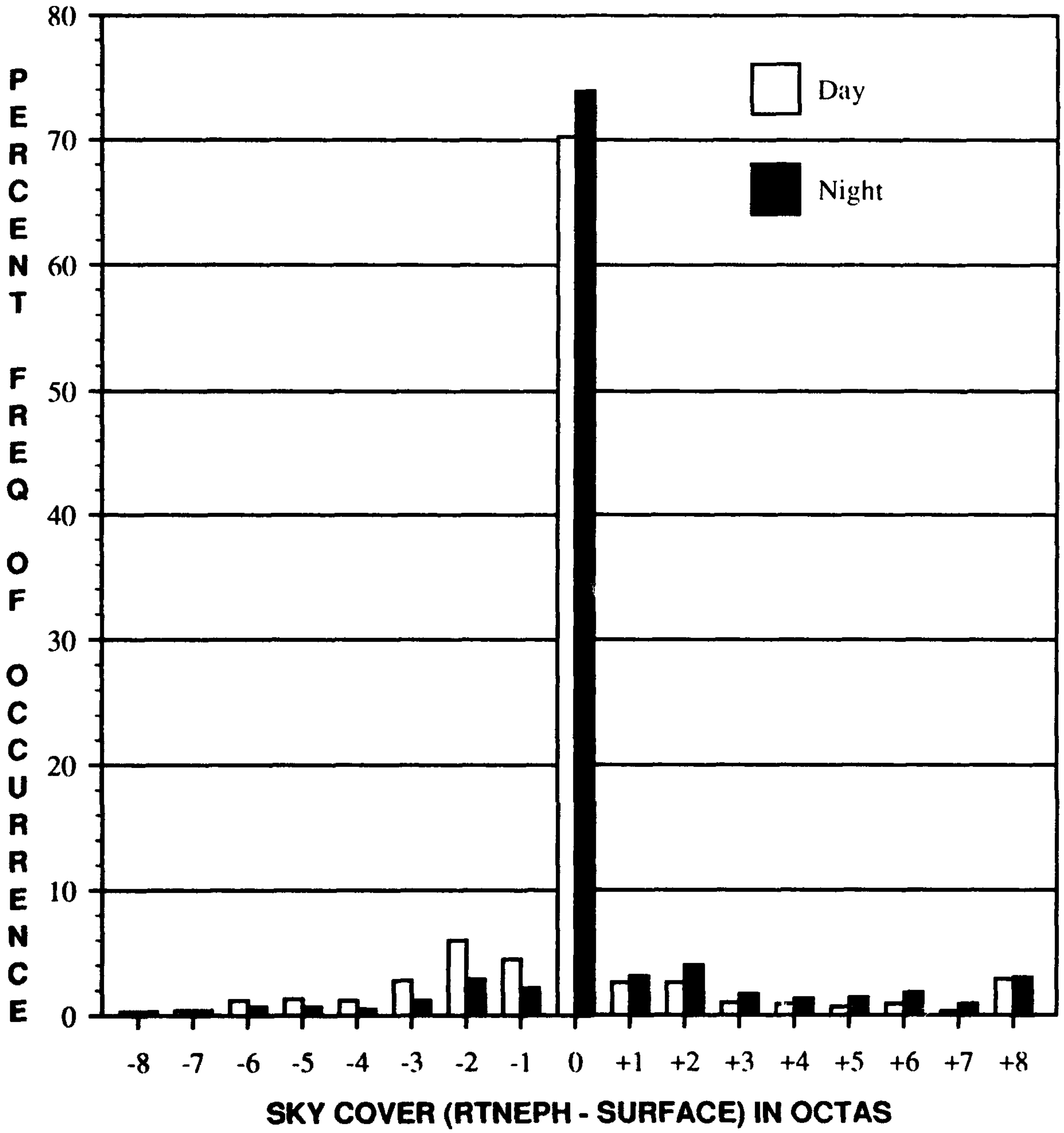

Figure 14. Comparison of Day/Night RTNEPH minus Surface Observations, mid-Latitudes, Summer.

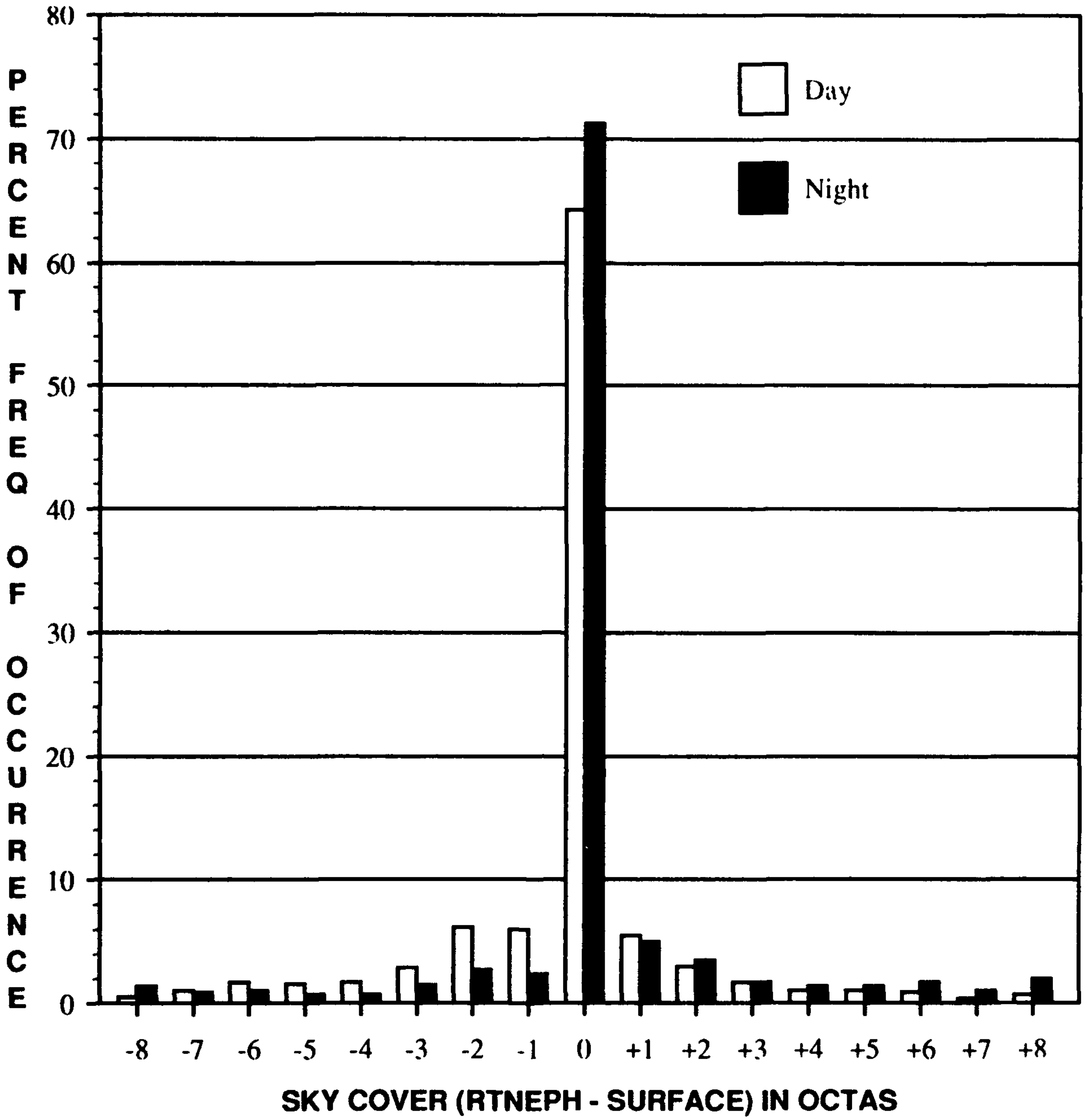

Figure 15. Comparison of Day/Night RTNEPH minus Surface Observations, mid-Latitudes, Autumn.

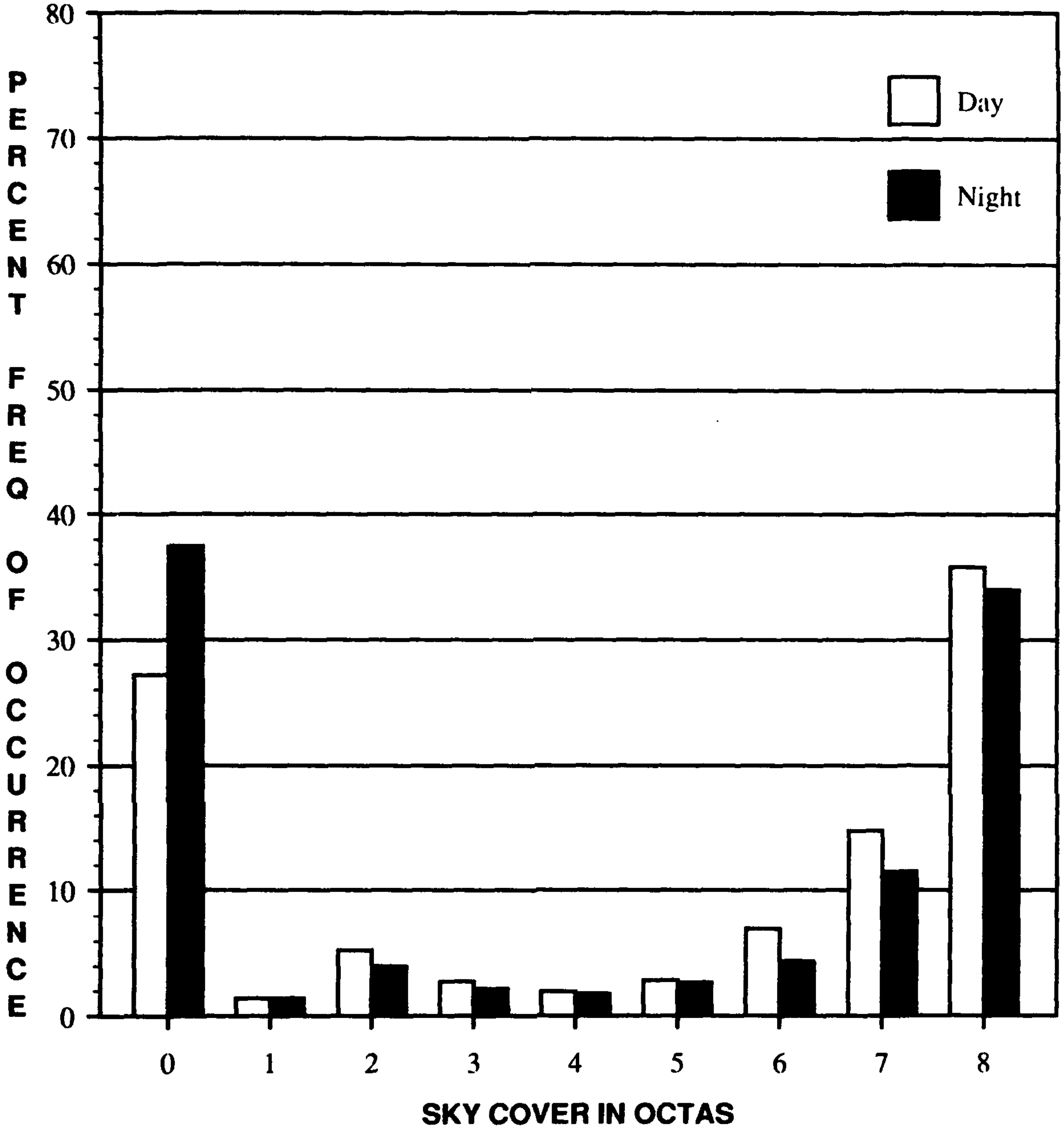

Figure 16. Comparison of Day/Night Stratification for RTNEPH, Mid-Latitudes, Winter.

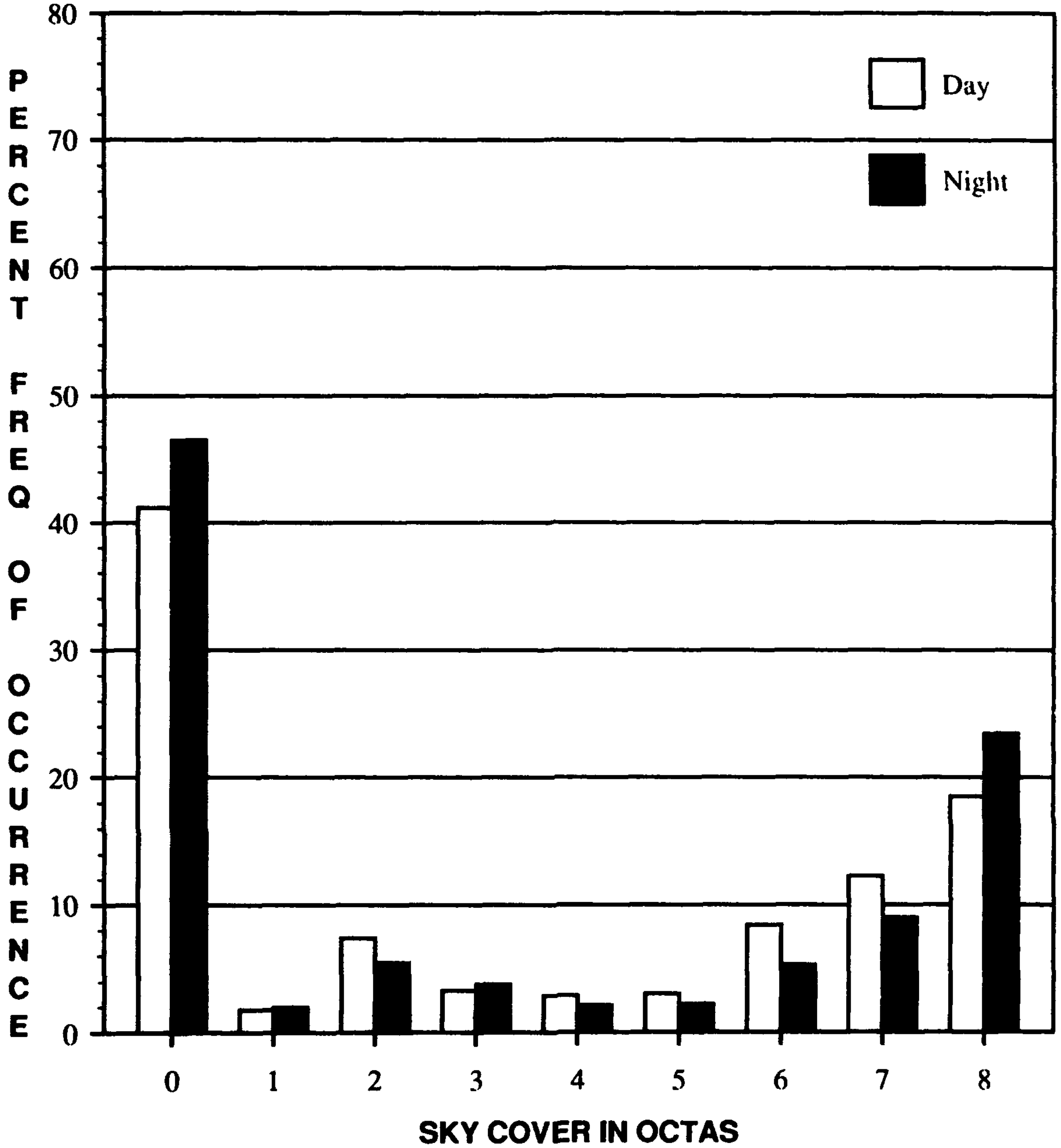

Figure 17. Comparison of Day/Night Stratification for RTNEPH, Mid-Latitudes, Spring.

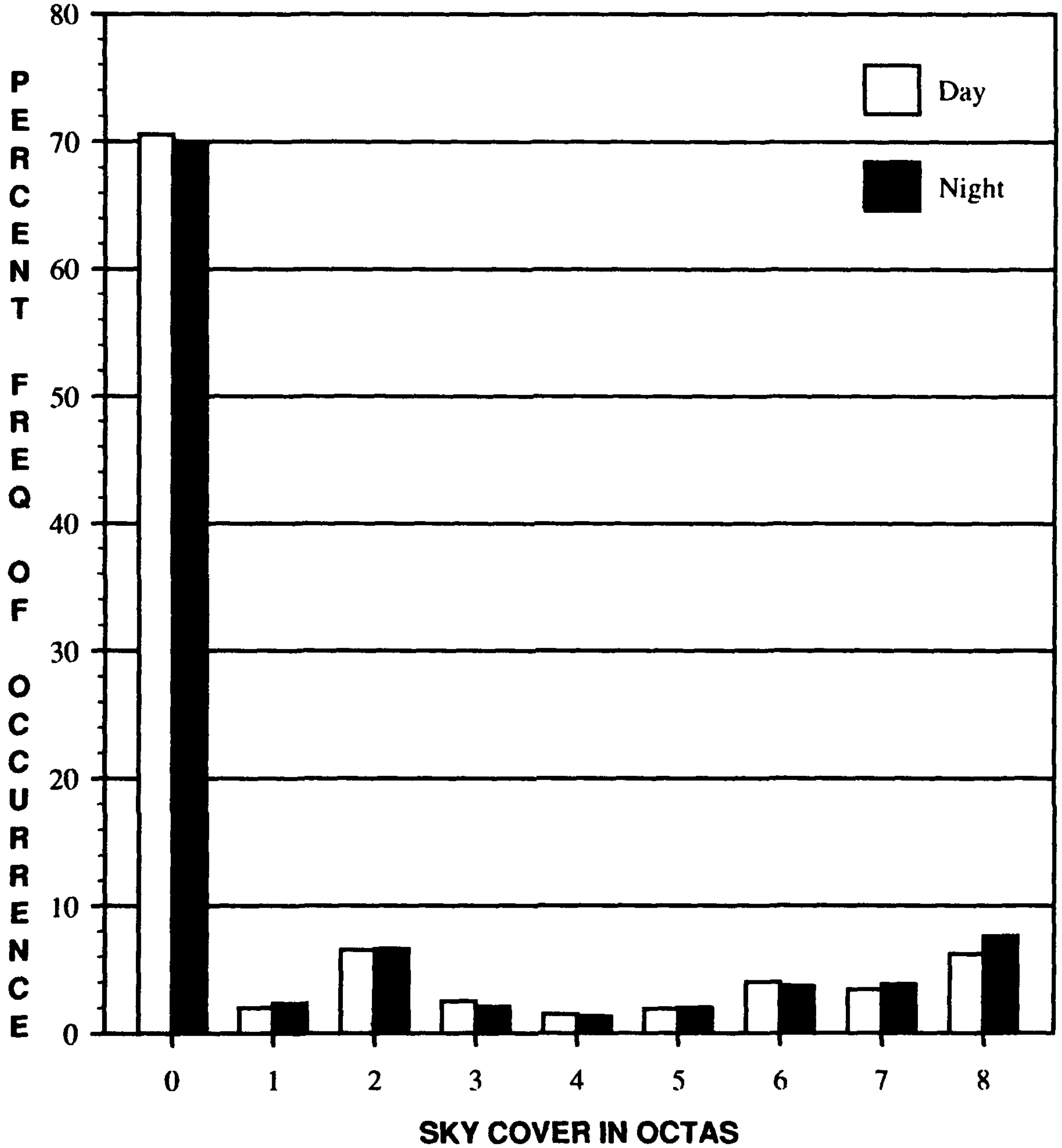

Figure 18. Comparison of Day/Night Stratification for RTNEPH, Mid-Latitudes, Summer.

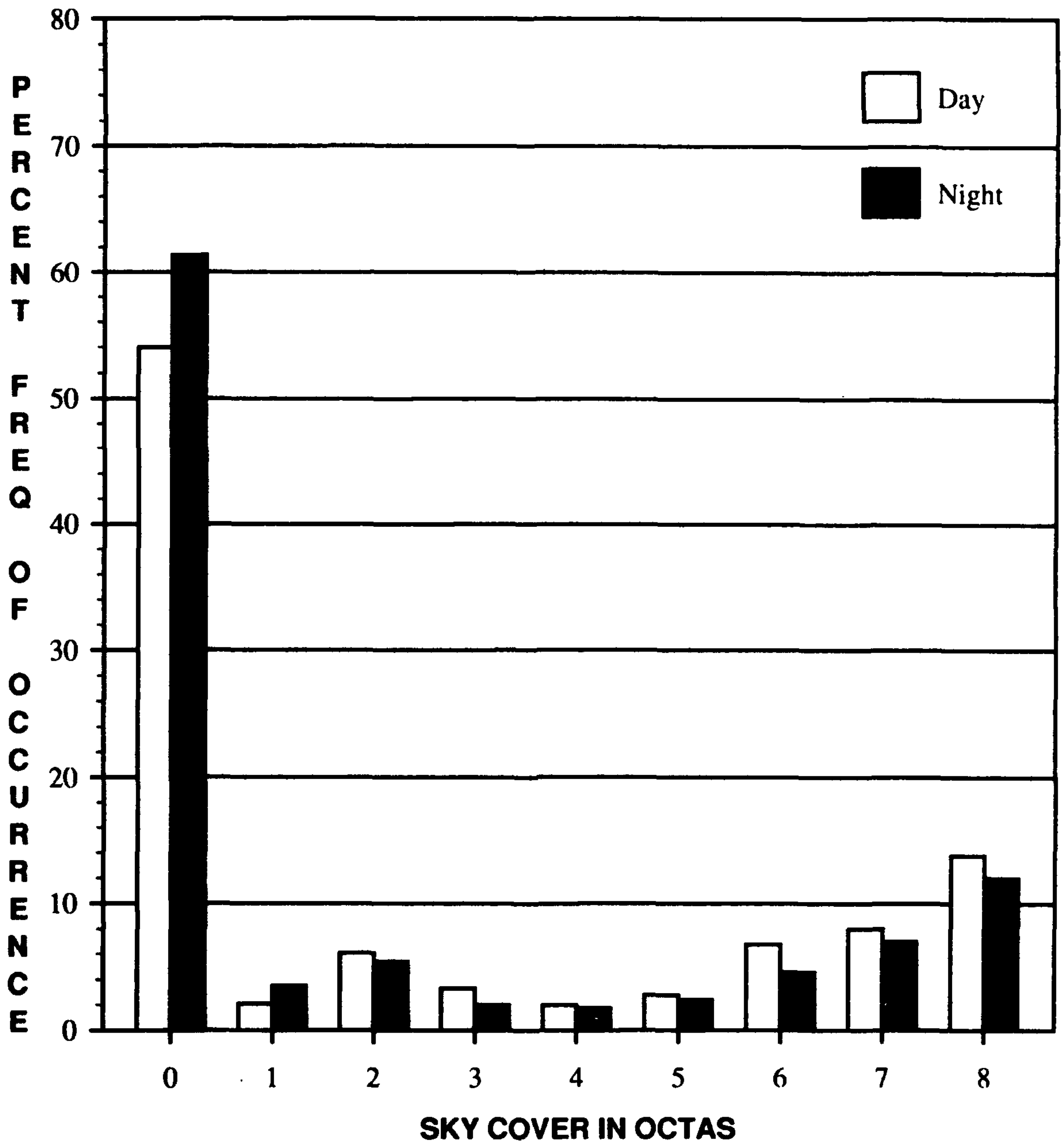

Figure 19. Comparison of Day/Night St ıtification for RTNEPH, Mid-Latitudes, Autumn.

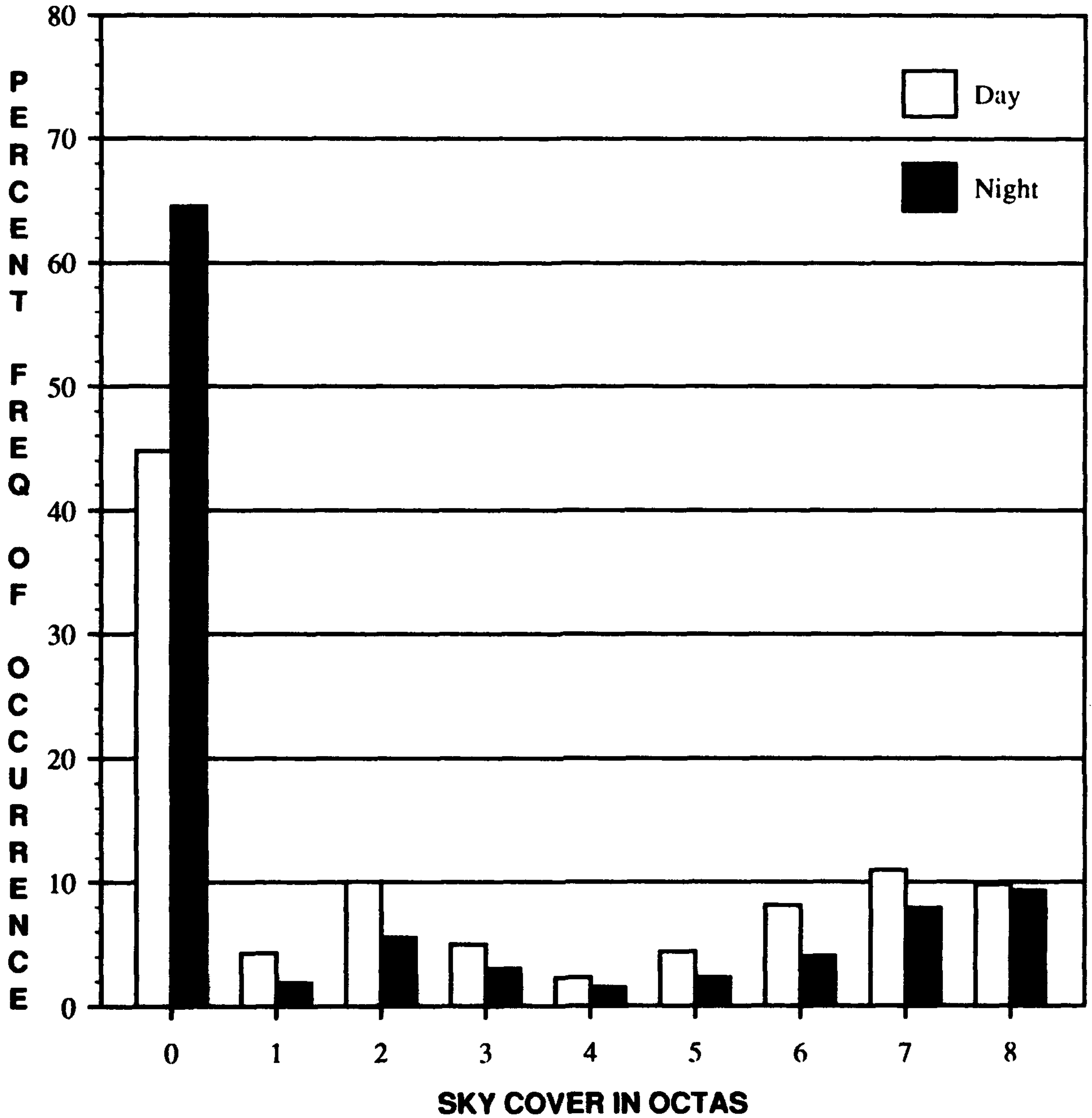

Figure 20. Comparison of Day/Night Stratification for Surface Databases, Mid-Latitudes, Winter.

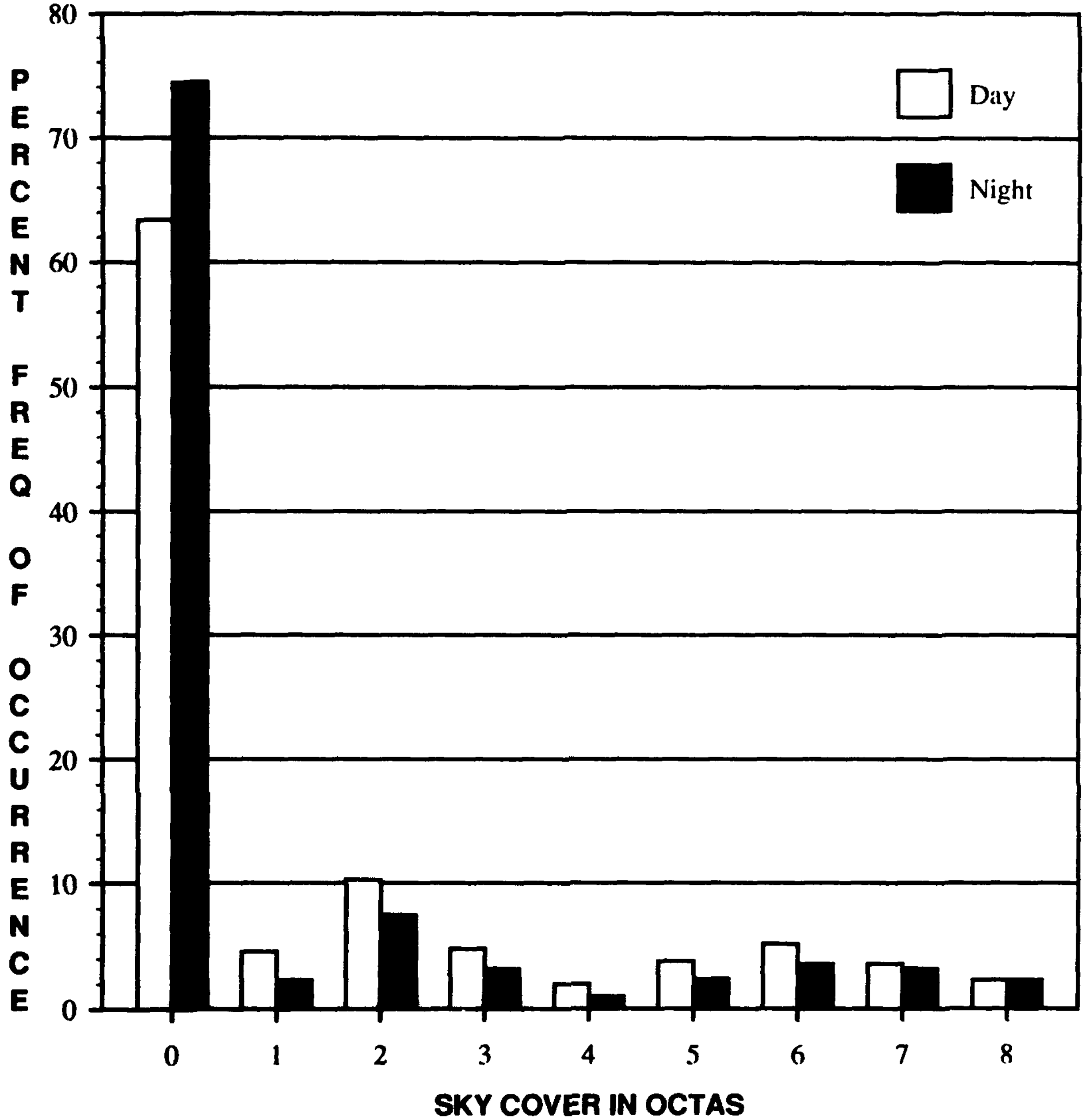

Figure 21. Comparison of Day/Night Stratification for Surface Databases, Mid-Latitudes, Spring.

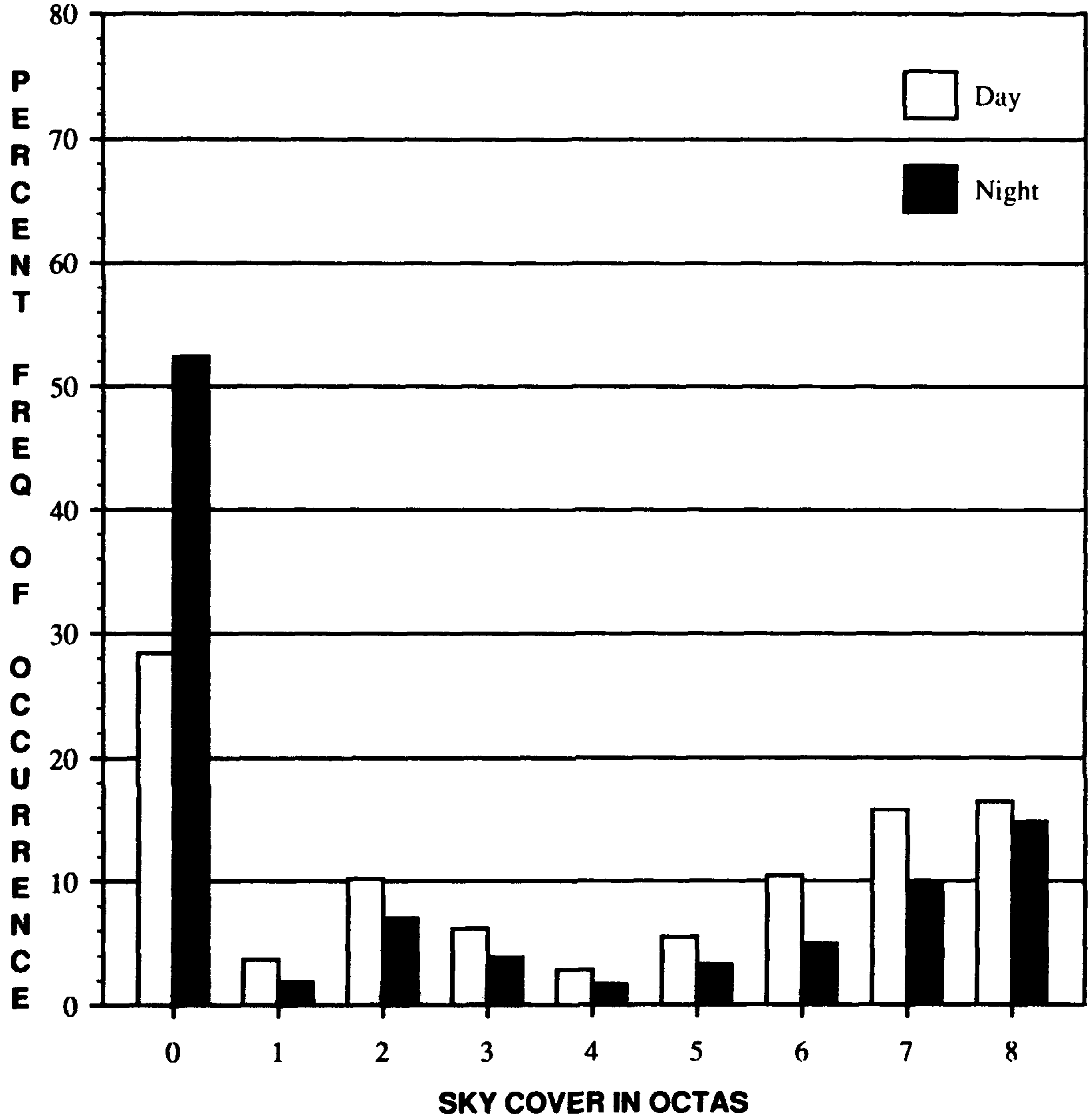

Figure 22. Comparison of Day/Night Stratification for Surface Databases, Mid-Latitudes, Summer.

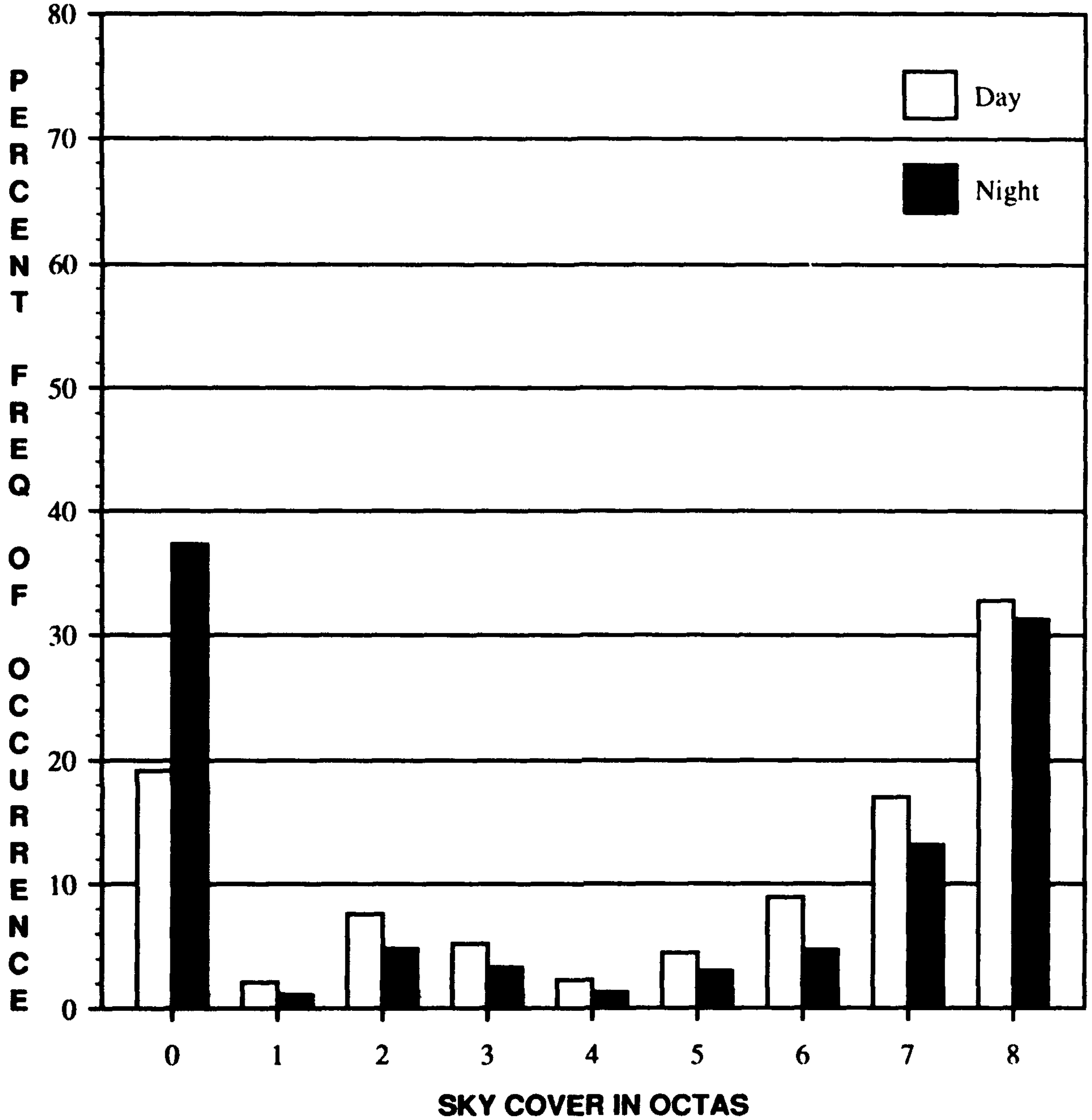

Figure 23. Comparison of Day/Night Stratification for Surface Databases, Mid-Latitudes, Autumn.

5.3 Time-Lag Comparison. The global RTNEPH minus surface TCC differences were grouped by data age as described in Section 4.4 and stratified by season. The resultant frequency distributions for the time-lag hours are plotted in Figures 24-27. The RTNEPH TCC amounts did not show significant differences, even in the 19-24 hour group. The percentage of observations with zero error is smallest in the 4-6 hour range; it actually increases for the 19-24 hour range to nearly the value for the 0-3 hour range. This is contrary to expectation, but it may be the result of diurnal effects such as low clouds, which dissipate during the day but often return again the same time the following day. Also, a significant fraction of the ± 7 and ± 8 errors are in the 19-24 hour interval. This is more in line with expectation. All this data, however, may have been affected by the bogusing discussed in Section 3.4. We don't know to what extent bogusing changed the older data.

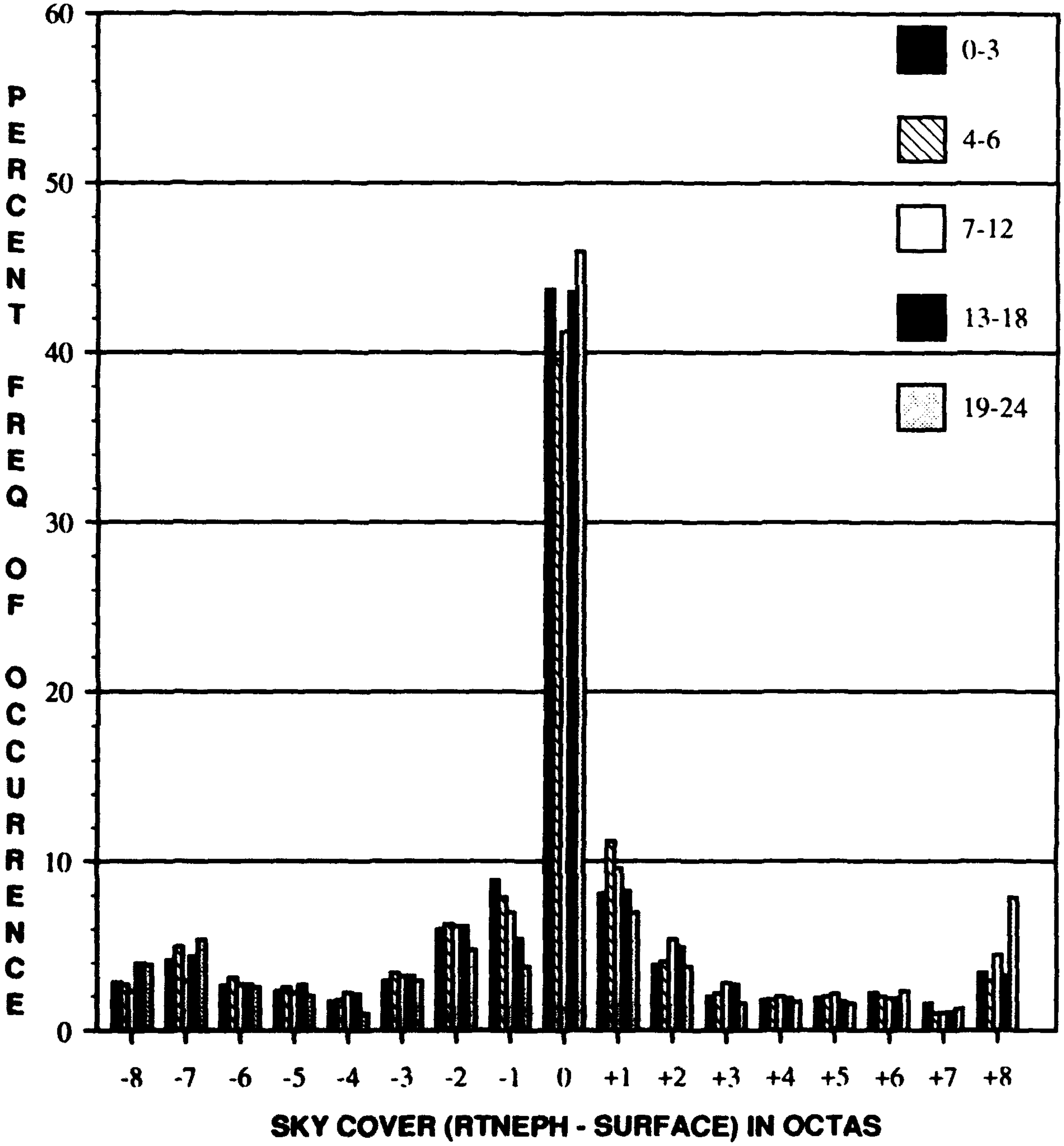

Figure 24. Comparison of RTNEPH and Surface Report Differences for Different Time-Lag Hour Groups, All Latitudes, Winter.

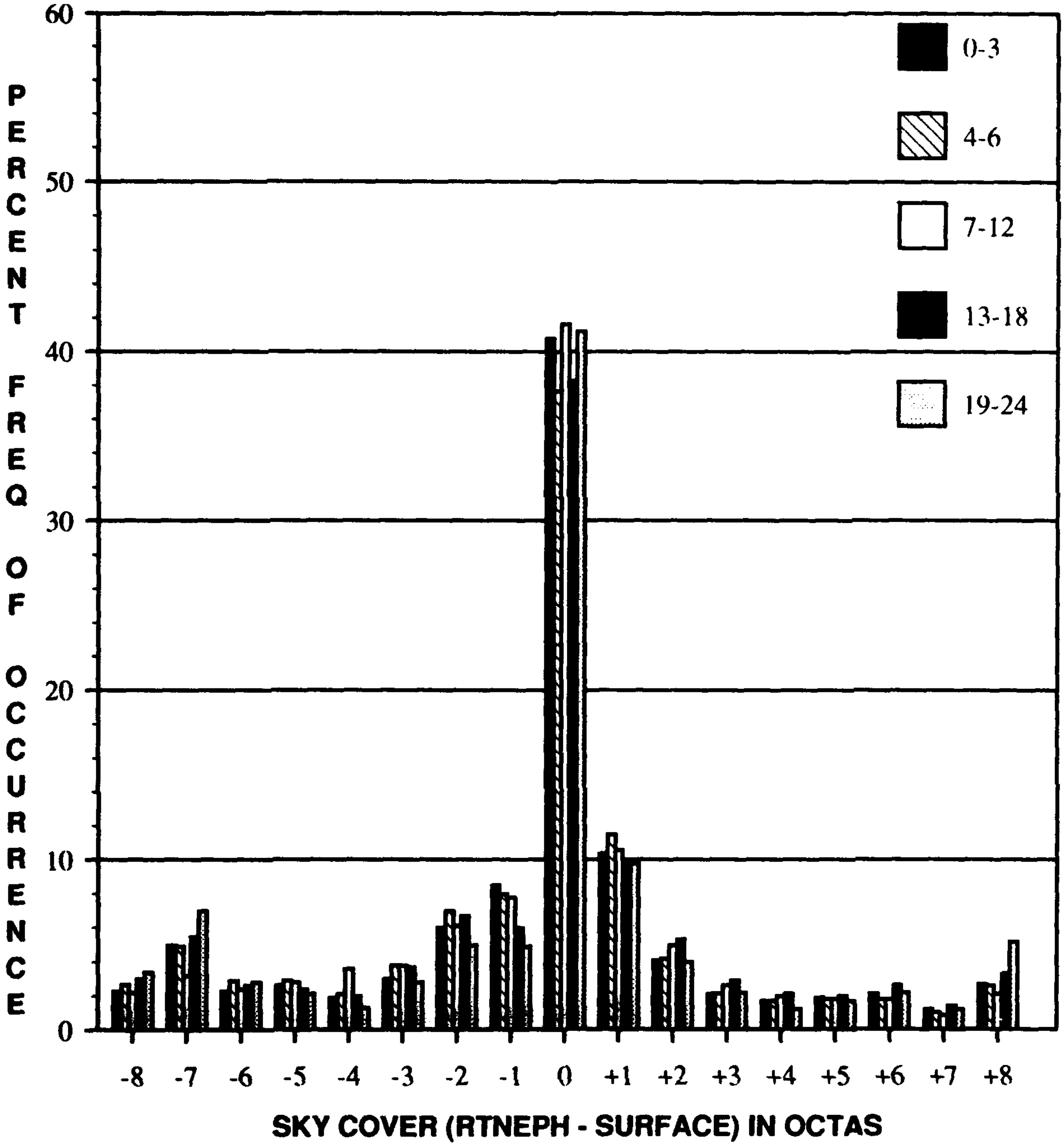

Figure 25. Comparison of RTNEPH and Surface Report Differences for Different Time-Lag Hour Groups, All Latitudes, Spring.

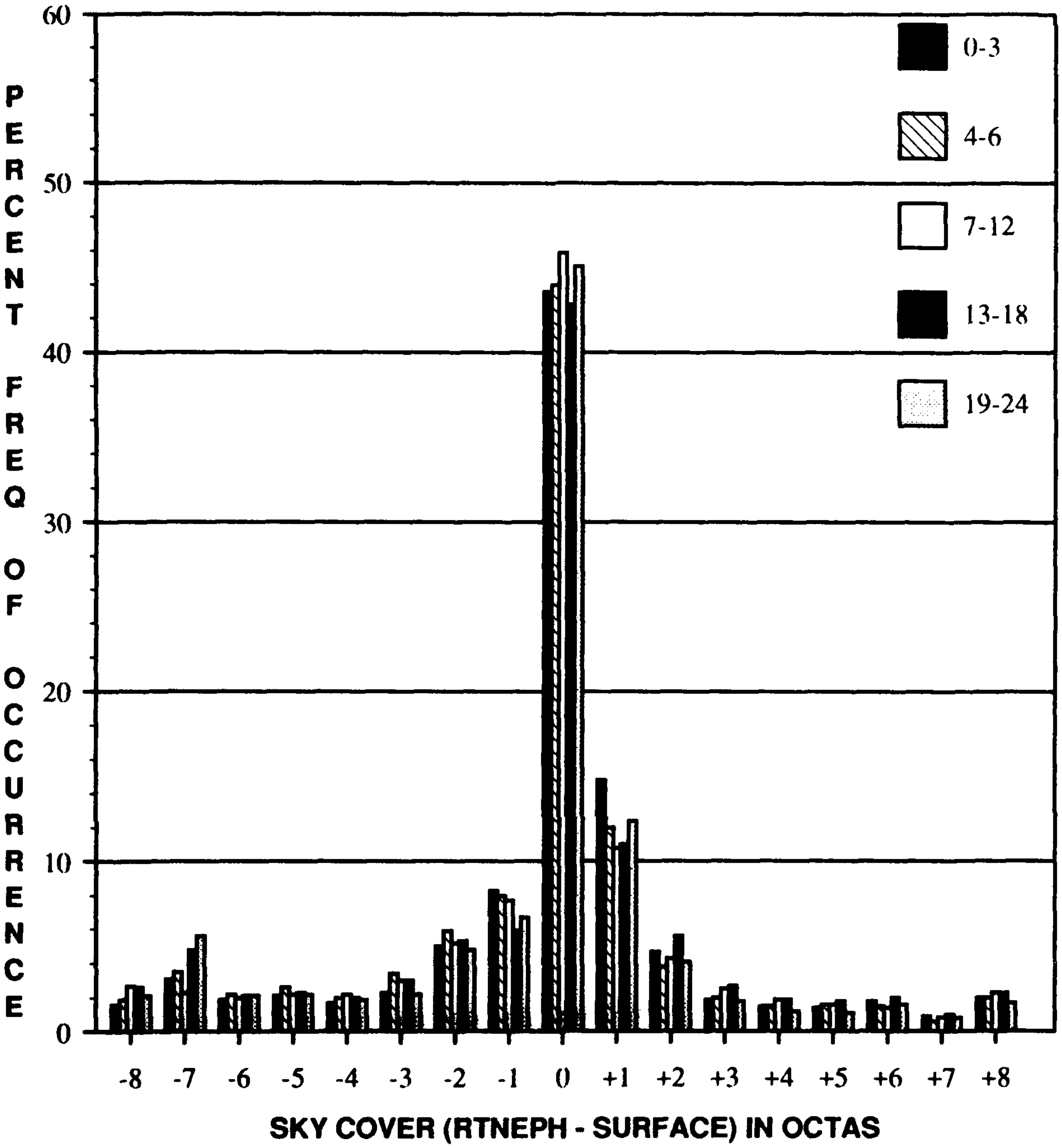

Figure 26. Comparison of RTNEPH and Surface Report Differences for Different Time-Lag Hour Groups, All Latitudes, Summer.

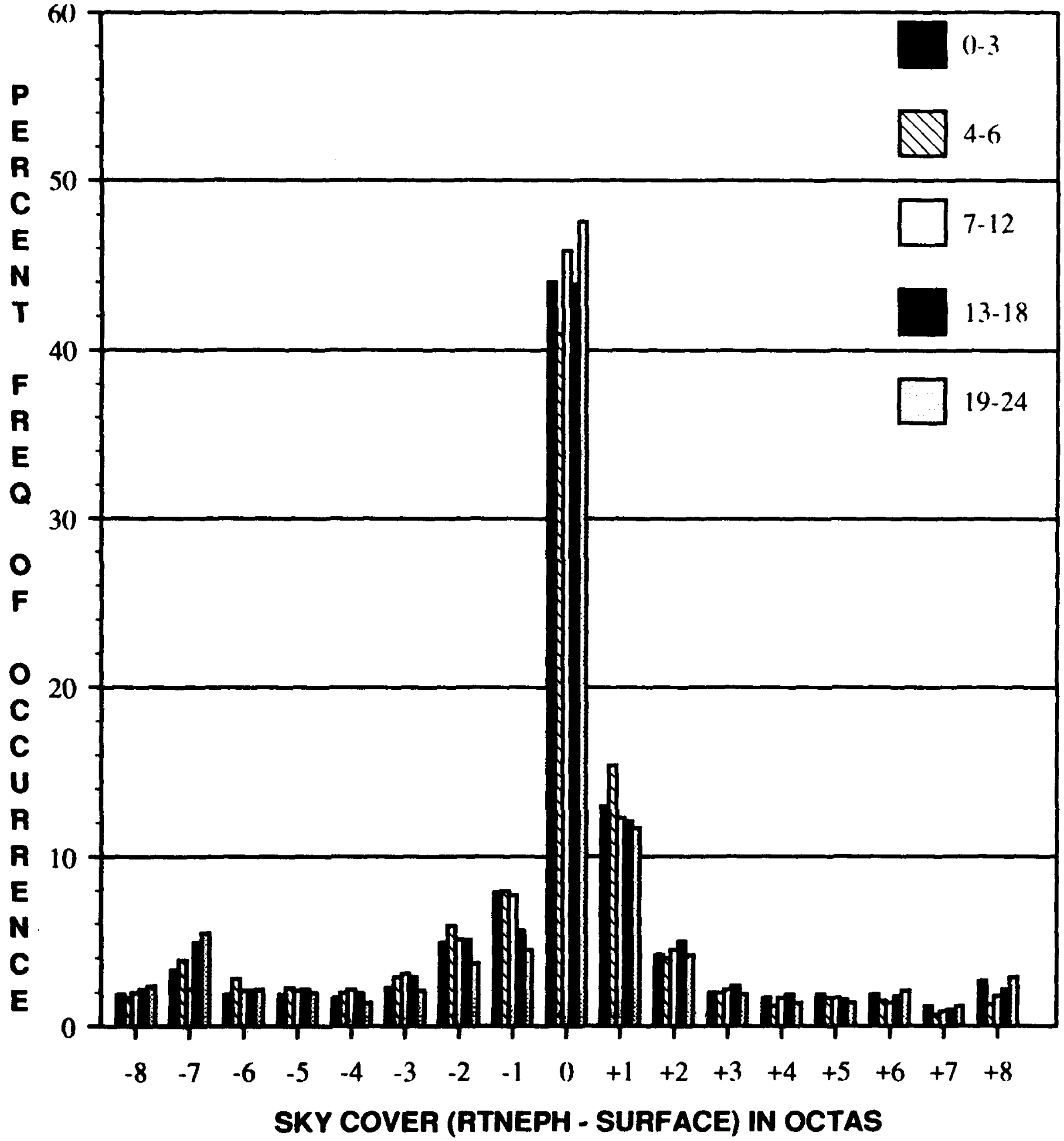

Figure 27. Comparison of RTNEPH and Surface Report Differences for Different Time-Lag Hour Groups, All Latitudes, Autumn.

6. STATISTICAL TESTS

Three statistical tests were used to evaluate the differences between the RTNEPH and surface cloud-cover observations. The test results can be used to provide an estimate of reliability for the TCC amount in the RTNEPH analysis. We used the t-test, the chi-square test, and the Spearman correlation coefficient.

6.1 T-Test. Most statistical tests are based on the assumption that data are normally distributed; cloud cover distributions, however, are not. According to Box et al. (1978), the t-test is insensitive to the normality assumption. When the distribution is non-normal, the distribution of the sample means will not be exactly normal. However, due to the central limit theorem, the distribution of the sample means will tend toward normality as the sample size increases. Box et al. demonstrated that the significance level of the t-test is barely affected by dramatic changes in the parent distribution. Hays and Winkler (1971) further pointed out that while the derivation of the t-distribution requires the assumption of normality, in practice, the t-distribution may be applied when the parent distribution is non-normal, provided that the random sample size is moderately large. Since this study uses random samples of 5,000, we believe the results of the t-test are valid and require no caveat.

Tables 3-5 summarize the results of each test. The t-test evaluates the null hypothesis that the mean difference between the RTNEPH and surface TCC amounts is zero. This test does not evaluate the quality of any randomly selected observation; instead, it assesses the agreement of the data as a whole. If the mean difference is zero, then the sign of the difference between any given observation pair should be randomly plus or minus; i.e., the difference is unbiased. If the t-test rejects the null hypothesis, it implies a bias in the differences. The accept/reject threshold was based on a 5% level of significance. For the mid-latitudes and tropics, in each season except winter in the tropics, the null hypothesis was accepted. During winter in the tropics and for all four seasons at the polar latitudes, the null hypothesis was rejected, implying a bias in the data.

TABLE 3. Polar Latitude Statistical Test Results (by Season).

SEASON	T-TEST	CHI-SQUARED	PHI COEF	CORRELATION COEFFICIENT
WINTER	Reject	Different	0.32	0.30
SPRING	Reject	Different	0.35	0.27
SUMMER	Reject	Different	0.43	0.34
AUTUMN	Reject	Different	0.35	0.35

TABLE 4. Mid-Latitude Statistical Test Results (by Season).

SEASON	T-TEST	CHI-SQUARED	PHI COEF	CORRELATION COEFFICIENT
WINTER	Accept	Different	0.17	0.60
SPRING	Accept	Different	0.19	0.63
SUMMER	Accept	Different	0.17	0.71
AUTUMN	Accept	Different	0.14	0.67

TABLE 5. Tropical Latitude Statistical Test Results (by Season).

SEASON	T-TEST	CHI-SQUARED	PHI COEF	CORRELATION COEFFICIENT
WINTER	Reject	Different	0.20	0.52
SPRING	Accept	Different	0.22	0.50
SUMMER	Accept	Different	0.10	0.52
AUTUMN	Accept	Different	0.12	0.51

6.2 Chi-Square Test. The chi-square test is used to evaluate the null hypothesis that two frequency distributions are similar. Brooks and Carruthers (1953) state that any two observed distributions may be compared with the chi-square test without reference to the theoretical forms of the distributions. They further state that a useful application of the test in meteorology is testing the similarity of frequency distributions of two or more sets of observations. In this case, we compared the frequency distributions of cloud cover, derived from the RTNEPH analysis, with surface observations. In all cases, at the 5% level of significance, the null hypothesis was rejected. Thus the distributions are statistically different.

Because the chi-square test is very sensitive to sample size, and to evaluate the degree to which the distributions differ, we use the phi coefficient (the square root of the chi-square statistic divided by the sample size). This coefficient ranges from -1 to +1. Values close to zero indicate the distributions are nearly identical, while those approaching either 1 or -1 are significantly distinct. In most of the cases, the phi coefficient was less than or equal to 0.20, implying a large degree of similarity in the two distributions. However, at the polar latitudes, values ranged from 0.32 to 0.43. This suggests there are some noticeable differences between the RTNEPH and surface data in the polar latitudes.

6.3 Spearman Correlation Coefficient Test. The final test was the Spearman correlation coefficient, a non-parametric test (Conover, 1990) that determines how well the individual observations are correlated. The more familiar form of the correlation coefficient is the Pearson product moment, which was not used because it is based on an assumption of normality and is too sensitive to non-normality.

The values for the Spearman coefficient also range from -1.0 to 1.0. In all cases, the samples are positively correlated with coefficient values hovering around 0.5. The mid-latitudes performed best, with correlation values ranging from .60 to .71 depending on the season. Once again, the polar region did not have as favorable results as the other latitudinal regions.

6.4 Test Conclusions. Tables 3-5 indicate that seasons do play a significant role in the accuracy of the RTNEPH total cloud-cover analysis. The two sources are in closest agreement during the summer months. The fact that the greatest problems in the data occur at the polar latitudes suggests that the RTNEPH analysis does in fact have difficulty separating ice/snow cover from cloud-cover. In the tropics, winter differences reveal a positive bias (RTNEPH TCC greater than surface TCC). This may be a result of small-scale clouds. If small-scale, evenly distributed clouds are present, they can inundate the coarser pixels comprising the RTNEPH grid area, resulting in an overestimate of TCC. In any event, the observed bias is small, averaging only about 1 octa.

Overall, the test results are consistent. Three fundamental tests were conducted to evaluate different aspects of the comparison between the RTNEPH and surface total cloud-cover reports. They point to good meteorological agreement for TCC between the two databases. We must use caution, however, because statistics can often be misleading even when using large sampling sizes. For example, if we collected cloud data at a location for one complete year and examined it against cloud data for the same location the following year, we would probably conclude that the data was from different locations. The reason for this is the large year-to-year variability in cloud-cover that occurs at any one location.

7. WHOLE SKY IMAGERY COMPARISON

To conclude our study of the TCC analysis, we compared it with whole sky imagery (WSI) data. The Phillips Laboratory Geophysics Directorate provided WSI data for Malabar, Florida, 5 miles NE of Melbourne Regional Airport. The data was only available from 6 October 1989 to 3 April 1990 for 6 hours either side of local noon. Surface observations were obtained from Melbourne Regional Airport. Because of the limited amount of WSI data, this point study is only included to point out a weakness in the RTNEPH model analysis over countries such as the United States.

For this part of the study, RTNEPH data was not independent from surface observations, and we expected very high agreement between them. The RTNEPH and WSI data were independent. Figures 28-30 show the results for three seasons--summer is not included. Analysis of the surface observations and RTNEPH data (from the grid area closest to the WSI sensor) clearly showed the model directly used surface reports from Melbourne Regional Airport for this grid area; therefore, it is not surprising that the RTNEPH and surface observations compared favorably. This was not the case for RTNEPH and WSI data for the same time period. Because the airways reporting code (not synoptic) is used at Melbourne, TCC resolution was degraded from octas to one of four reporting categories: clear, scattered, broken, or overcast.

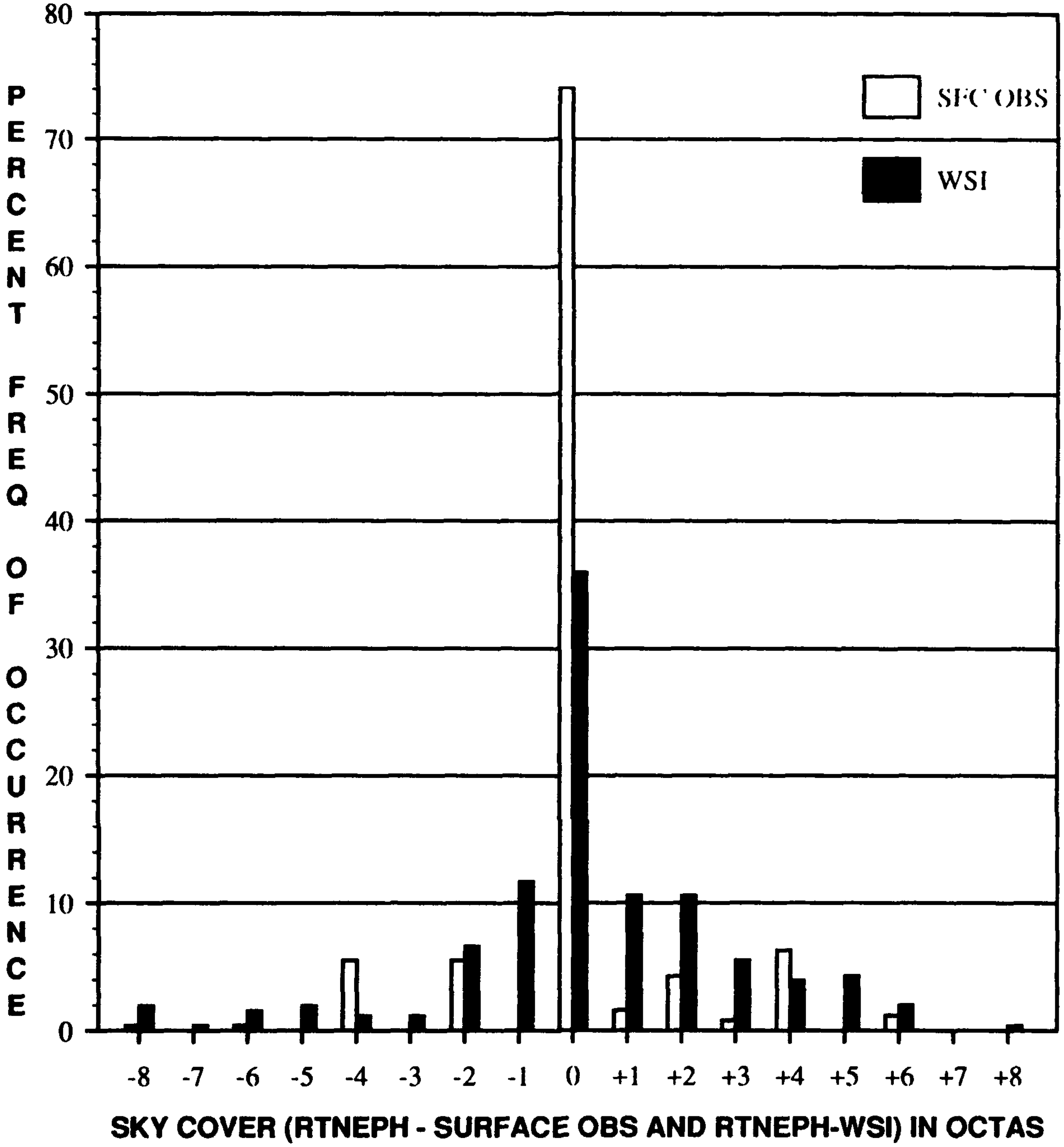

Figure 28. Comparison of RTNEPH WSI and Surface Reports Over Malabar, FL, Winter.

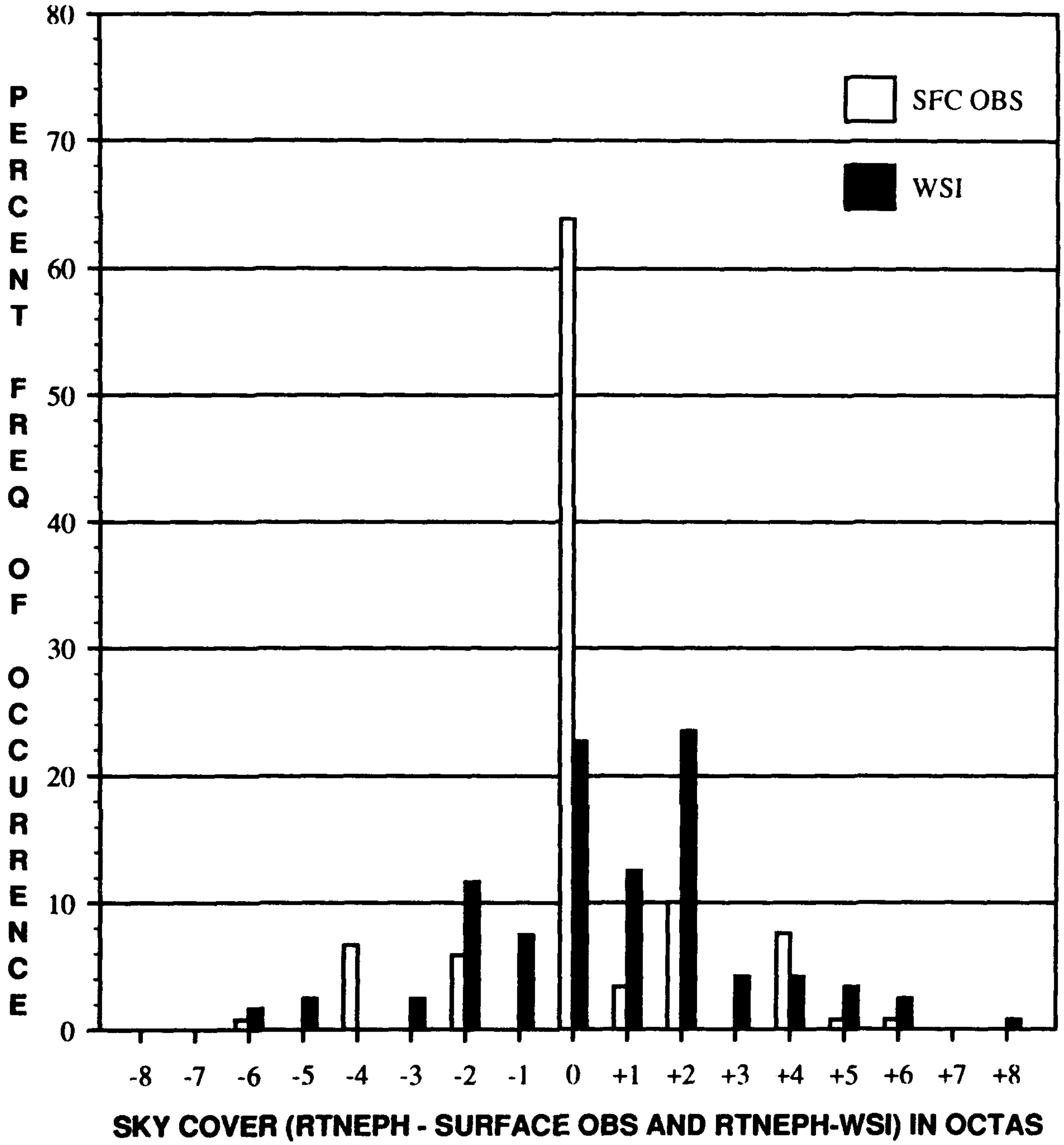

Figure 29. Comparison of RTNEPH WSI and Surface Reports Over Malabar, FL, Spring.

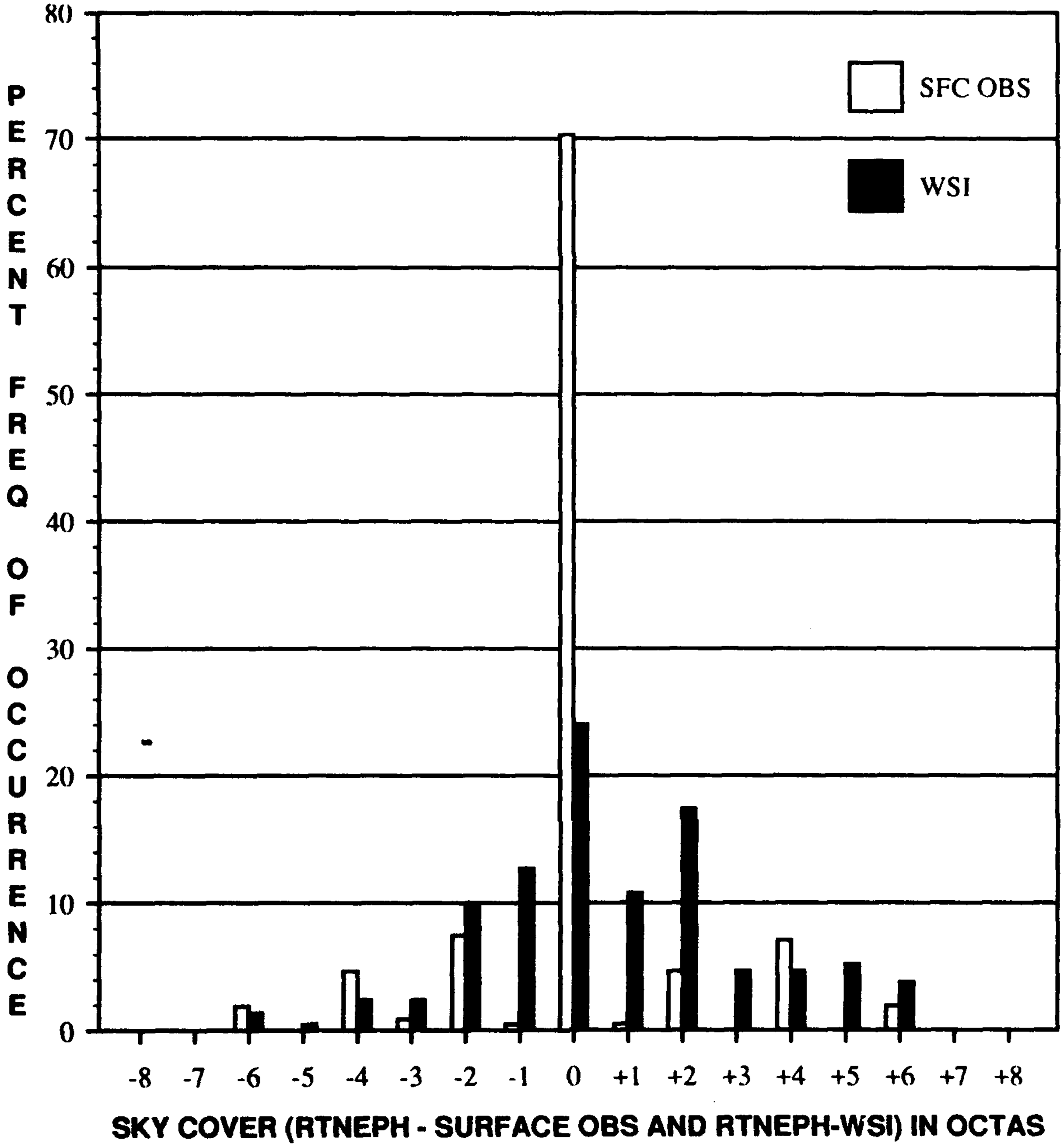

Figure 30. Comparison of RTNEPH WSI and Surface Reports Over Malabar, FL, Autumn.

WSI imagery is recorded as a percentage of sky cover. Since the RTNEPH relies heavily on surface observations, nearly all cloud-cover amounts are either 0, 25, 75, or 100%. As a result, the RTNEPH-WSI comparison was poor, implying that RTNEPH total cloud-cover amounts over the United States (and other areas with widespread airways code reporting) have poor resolution. Since the other stratifications showed the satellite to be a reliable data source, it might be advantageous for RTNEPH to record cloud-cover over the U.S. using only satellite data (especially if surface-based observed data is other than clear or overcast). However, one must first consider the persistence of the satellite-derived observations against the coarser resolution of airways observations.

8. CONCLUSIONS

Independent observations of total cloud-cover made from surface-based observers show that satellite-derived cloud-cover amounts in the RTNEPH analysis have a large degree of precision. The largest discrepancies appear in polar regions, where the RTNEPH analysis tends to underestimate observed cloud-cover, probably due to difficulties in discriminating between low cloud and snow- or ice-covered ground. A major revision in the RTNEPH algorithm is scheduled for implementation in 1991; the changes include the use of microwave channels for estimating surface temperatures. We believe that this and other changes may significantly improve detection of clouds over snow-covered surfaces. Actually, microwave capability for estimating surface temperatures has been available since 1989, but it was turned off due to problems with SSM/I data. Future DMSP satellites should have those problems corrected, and with RTNEPH stratifying the data by day/night/snow/land/water/ice/satellite, they should provide better information for detecting clouds. A small bias of over-reporting of cloud-cover was also noted for the tropical latitudes during the winter months.

The effect of the age of the RTNEPH data produced unexpected results. The poorest comparisons, on average, were associated with data 4-6 hours old. Older data improved slightly with age, with the 19-24 hour group having a similar frequency of a zero difference (RTNEPH minus surface) as for the 0-3 hour group. We attribute this to diurnal effects. The 19-24 hour range did show the greatest frequency for the absolute value of this difference being greater than or equal to 7 octas. Overall, however, data age appears to be a minor problem.

Next we examined day and night observations for evidence of bias. It appears that an observer is more likely to report clear skies at night when, in fact, scattered clouds are detected by the RTNEPH analysis. However, the overall difference in the two cloud-cover amounts is generally 2 octas or less. The results show that RTNEPH and the surface observer both suffer disabling effects at night. Both report more clear conditions and they agree with each other very well at night.

Research data sets such as the whole sky imagery data are good sources of objective cloud-cover data, and would be ideal for evaluating RTNEPH analyses. Unfortunately, these data are only available for a few locations in the United States, where the resolution of the RTNEPH cloud-cover analyses are poor due to the use of the airways reporting code. It might be advantageous for the RTNEPH model to record cloud cover over the U.S. using only satellite data if an airways report contains scattered or broken conditions. In addition, we believe testing of observer-based TCC is inadequate. Perhaps AWS might work with NWS to acquire synoptic reports from or near WSI sites. This would enable significantly enhanced studies of observer precision.

The objective of this study was to quantitatively evaluate the total sky-cover analysis and determine its precision. It suggests that while the overall quality of the RTNEPH total sky-cover analysis is good, that conclusion is highly dependent on the operational needs of the data user. Figures 6-9 show the frequency distribution of differences (or errors) between RTNEPH and surface reports. Confidence limits of the data can also be calculated using these graphs. Using Figure 6, we can state that the RTNEPH analysis is accurate to within +/- 2 octas 69% of the time averaged over the globe in winter. However, we can also state that it is totally *inaccurate* (error of 7 or 8 octas) 12.5% of the time. The acceptability of these accuracies, as well as the errors, is user-dependent. In general, however, there was a close agreement between RTNEPH data and surface observations except in the polar regions.

BIBLIOGRAPHY

Box, G.E.P., W.G. Hunter, *Statistics for Experimentors,* John Wiley and Sons, New York, 1978.

Brooks, C.E.P., and N. Carruthers, *Handbook of Statistical Methods in Meteorology,* Her Majesty's Stationary Office, London, 1953.

Conover, W.J., *Practical Nonparametric Statistics,* John Wiley and Sons, New York, 1980.

Hays, W.L. and R.L. Winkler, *Statistics, Probability, Inference, and Decision,* Holt, Rinehart, and Winston, Inc., New York, 1971.

Kiess, R.T. and W.M. Cox, *The AFGWC Automated Real-Time Cloud Analysis Model.* AFGWC/TN-88/001, AFGWC, Air Weather Service, Offutt AFB, NE, 1988.

Snow, J.W., *Modeling The Variation of Cloud Cover with View Angle Using Space Shuttle Cloud Imagery,* GL-TR-90-0130, Environmental Research Paper No 1064. Geophysics Laboratory, Hanscom AFB, MA 01731-5000, 1990.

ACRINABS

ACRINABS	Acronyms, initialisms, and abbreviations
AFGWC	Air Force Global Weather Central
AWS	Air Weather Service
Neph	Nephanalysis
NH	Northern hemisphere
NM	Nautical Mile
RTNEPH	Real-Time Nephanalysis
SH	Southern hemisphere
SSM/I	Special Sensor Microwave Imager
TCC	Total cloud cover
3DNEPH	3-Dimensional Nephanalysis
WMO	World Meteorological Organization
WSI	Whole Sky Imagery

DISTRIBUTION

AWS//DO/XT, Scott AFB, IL 62225-5008 1
Det 1, HQ AWS, Pentagon, Wash DC 20330-6560 1
OL A, AFCOS, Ft Ritchie MD 21719-5010 1
CSTC/WE, PO Box 3430, Onizuka AFB, CA 94088-3430 1
OD-4/DX, Onizuka AFB, CA 94088-3430 1
Det 9, HQ AWS, PO Box 12297, Las Vegas, NV 89112-0297 1
1SSD/WE (Stop 77), Buckley ANG Base, Aurora, CO 80011-9599 1
OL-B, HQ AWS, Hanscom AFB, MA 01731-5000 1
OL-E, HQ AWS, Ft Leavenworth, KS 66027-5310 1
SSD/MWA, PO Box 92960, Los Angeles, CA 90009-2960 1
OL-H, HQ AWS, Ft Huachuca, AZ 85613-7000 1
OL-I, HQ AWS, Ft Monroe, VA 23651-5000 1
OL-K, HQ AWS, NEXRAD Opnl Support Facility, 1200 Westheimer Dr. Norman, OK 73069 1
OL-M, HQ AWS, McClellan AFB, CA 95652-5609 1
AFGWC/SYSE MBB39 106 Peacekeeper Dr Ste 2N3 Offutt AFB, NE 68113-4039 5
USAFETAC, Scott AFB, IL 62225-5438 6
1WW/DN, Hickam AFB, HI 96853-5000 1
    11WS/DON 6900 9th St Ste 205 Elmendorf AFB AK 99506-2250 1
    20WS/DON, APO AP 96328-5000 1
    30WS/DON, APO AP 96301-0420 1
2WW/DNC, Unit 3135, APO AE 09094-5000 1
    7WS/DON, APO AE 09403-5000 1
    28WS/DON, APO AE 09127-5000 1
    31WS/DON, APO AE 09136-5000 1
HQ SAC DOW 901 SAC Blvd STE M138 Offutt AFB, NE 68113-5340 1
2AF DOW, Beale AFB, CA 95903-5000 1
8AF DOW, Barksdale AFB LA 71110-5002 1
HQ ATC DOTW, Randolph AFB, TX 78150-5000 1
4WW/DN, Peterson AFB, CO 80914-5000 1
    2WS/DON, Andrews AFB, MD 20334-5000 1
5WW/DN, Langley AFB, VA 23665-5000 1
    1WS/DON MacDill AFB, FL 33608-5000 1
    3WS/DON, Shaw AFB, SC 29152-5000 1
    5WS/DON, Ft McPherson, GA 30330-5000 1
    25WS/DON, Bergstrom AFB, TX 78743-5000 1
MAC/XOW Scott AFB, IL 62225-5008 1
438 MAW/WXF, McGuire AFB, NJ 08641-5002 1
60 MAW/WXF, Travis AFB, CA 94535-5986 1
USTC J3/4 OW, Scott AFB, IL 62225-5000 1
3350 TCHTG/TTGU-W, Stop 62, Chanute AFB, IL 61868-5000 1
3395 TCHTG/TTKO-W, Keesler AFB, MS 39534-5000 1
COMNAVOCEANCOM, Code N312, Stennis Space Ctr, MS 39529-5000 1
COMNAVOCEANCOM (Capt Brown, Code N332), Stennis Space Ctr, MS 39529-5001 1
NAVOCEANO (Rusty Russum), Stennis Space Ctr, MS 39522-5001 1
NAVOCEANO, Code 9220 (Tony Ortolano),Stennis Space Ctr, MS 39529-5001 1
Maury Oceanographic Library (NOC), Code XJL, Stennis Space Ctr, MS 39529-5001 1
FLENUMOCEANCEN, Monterey, CA 93943-5006 1
NOARL West, Monterey, CA 93943-5006 1
Naval Research Laboratory, Code 4323, Washington, DC 20375 1
Naval Research Laboratory (Dr Riley), Code 4180, Washington, DC 20375 (SESS reports) 1

Naval Postgraduate School, Chmn, Dept of Meteorology, Code 63, Monterey, CA 93943-5000 1
Naval Oceanography Command Ctr, COMNAVMAR Box 12, FPO San Francisco, CA 96630-5000 1
Naval Oceanography Command Ctr, Box 31, USNAVSTA FPO New York, NY 09540-3000 1
Pacific Missile Test Center, Geophysics Division, Code 3253, Pt Mugu, CA 93042-5000 1
HQ NATO STAFFMET, IMS/OPS APO AE 09724 1
Dept of Commerce/NOAA/MASC Library MC5 (Jean Bankhead), 325 Broadway, Boulder, CO 80303 1
OFCM, Suite 900, 6010 Executive Blvd, Rockville, MD 20852 1
NOAA Library-EOC4WSC4, Attn: ACQ, 6009 Executive Blvd, Rockville MD 20852 1
NOAA/NESDIS (Attn: Nancy Everson, E/RA22), World Weather Bldg, Rm 703, Washington, DC 20233 1
NOAA/NESDIS (Attn: Capt Pereira, E/SP1), FB #4, Rm 0308, Washington DC 20233-0001 1
NGDC, NOAA, Mail Code E/GC4, 325 Broadway, Boulder, CO 80303-3328 1
Armed Forces Med Intel Agency, Info Svcs Div., Bldg 1607, Ft Detrick, Frederick, MD 21701-5004 1
PL OL-AA/SULLA, Hanscom AFB, MA 01731-5000 1
Atmospheric Sciences Laboratory (SLCAS-AT-AB), Aberdeen Proving Grounds, MD 21005-5001 1
Atmospheric Sciences Laboratory (SLCAS-AS-I 310-2c), White Sands Missile Range, NM 88002-5501 1
TECOM Atmos Sci Div, Attn: AMSTE-TC-AA (MacBlain), White Sands Missile Range NM 88002-5504 1
Army Missile Command, ATTN: AMSMI-RD-TE-F, Redstone Arsenal, AL 35898-5250 1
Army Test & Eval Cmd, ATTN: AMSTE-TC-AM (RE) TECOM Met Team, Redstone Arsenal, AL 35898-8052 1
Commander and Director, U.S. Army CEETL, Attn: GL-AE, Fort Belvoir, VA 22060-5546 1
6510 TESTW/TSTL, Edwards AFB, CA 93523-5000 1
RL/DOVL, Bldg 106, Griffiss AFB, NY 13441-5700 1
AFESC/RDXT, Bldg 1120, Stop 21, Tyndall AFB, FL 32403-5000 1
Technical Library, Dugway Proving Ground, Dugway, UT 84022-5000 1
NWS W/OSD, Bldg SSM C-2 East-West Hwy, Silver Spring, MD 20910 1
NCDC Library (D542X2), Federal Building, Asheville, NC 28801-2723 1
NIST Pubs Production, Rm A-405, Admin Bldg, Gaithersburg, MD 20899 1
DTIC-FDAC, Cameron Station, Alexandria, VA 22304-6145 2
AUL/LSE, Maxwell AFB, AL 36112-5564 1
AWSTL, Scott AFB, IL 62225-5438 50